Received: 25 February 2022 | Accepted: 16 November 2022

DOI: 10.1111/nrm.12363

Natural Resource Modeling WILEY

Time delays and pollution in an open-access fishery

Harald Bergland[1] | **Purnedu Mishra**[2] | **Pål Andreas Pedersen**[3] | **Arkadi Ponossov**[2] | **John Wyller**[2]

[1]School of Business and Economics, Campus Harstad, University of Tromsø - The Arctic University of Norway, Harstad, Norway

[2]Department of Mathematics, Faculty of Science and Technology, Norwegian University of Life Sciences, Ås, Norway

[3]Nord University Business School, Bodø, Norway

Correspondence
Purnedu Mishra, Department of Mathematics, Faculty of Science and Technology, Norwegian University of Life Sciences, P.O. Box 5003, Ås N-1432, Norway.
Email: purnedu.mishra@nmbu.no

Funding information
Norges Forskningsråd, Grant/Award Number: 239070.; Norges Miljø- og Biovitenskapelige Universitet

Abstract

We analyze the impacts of pollution on fishery sector using a dynamical system approach. The proposed model presupposes that the economic development causes emissions that either remediate or accumulate in the oceans. The model possesses a block structure where the solutions of the rate equations for the pollutant and the economic activity act as an input for the biomass and effort equation. We also account for distributed delay effects in both the pollution level and the economic activity level in our modeling framework. The weight functions in the delay terms are expressed in terms of exponentially decaying functions, which in turn enable us to convert the modeling framework to a higher-order autonomous dynamical system by means of a linear chain trick. When both the typical delay time for the economic activity and the typical delay time for the pollution level are much smaller than the biomass time scale, the governing system is analyzed by means of the theory for singularly perturbed dynamical systems. Contrary to what is found for population dynamical systems with absolute delays, we readily find that the impact of the distributed time lags

is negligible in the long-run dynamics in this time-scale separation regime.

Recommendations for Resource Managers

- Resource managers should be aware of the dynamical interrelations between fisheries and pollution, also those that are time delayed.
- Time lags between biological, economic, and environmental variables are affecting the time paths of these variables.
- In the long run, the impact from distributed time lags have a negligible influence on the long-run dynamical evolution.
- Neither the past history of economic activities nor the past history of pollution growth can affect the fishery dynamics in the long run.
- More empirical and theoretical research are needed to increase our understanding of the interrelation between fisheries and pollution.

KEYWORDS

distributed delay systems, geometric perturbation theory, pollution, slow–fast fishery dynamics

1 | INTRODUCTION

Marine pollution is a widespread problem affecting the ocean health, the health of marine species, food security, and quality, and it contributes to climate change. As reported by Halpern et al. (2008), Islam and Tanaka (2004), Jones and Reynolds (1997), Todd et al. (2010), Vikas and Dwarakish (2015), and Lu et al. (2018), marine pollution is increasing and causes negative effects on commercial fisheries. A discussion of different forms of emission of pollution into the marine environment and their potential to be broken down can be found in Watson et al. (2016).

An interesting and early contribution discussing self-cleaning abilities of ecosystems can be found in Haavelmo (1971). Similar analyses of the self-cleaning models are found in Keeler et al. (1971), Strøm (1971), d'Arge (1971), and Smith (1972). More recently, similar models have been analyzed by several authors (see, e.g., Bergland et al., 2020, 2019; Chevé, 2000; El Ouardighi et al., 2014; Flaaten, 2018; Førsund & Strøm, 1980; Perman et al., 2011; Prieur, 2009; Tietenberg & Lewis, 2014; Toman & Withagen, 2000; Watson et al., 2016). Bergland et al. (2019) proposed a model to investigate the impact of pollution with self-cleaning ability and economic development on a modified fishery model. The current work extend this model to understand the impact of bioeconomic time delays.

In a dynamic analysis of the interaction between pollution and fisheries, possible time delays are relevant. For the self-cleaning ability of waste both the present state as well as the past history are expected to influence the ongoing remediation capacity. Also for the growth of fish resources it is reasonable to expect that pollution history matters. Furthermore, when it comes to both fishermen and consumers, their behavior is affected by the present and the former economic conditions.

Economists have for a long time been engaged in modeling time delays in macro- and microeconomic models to reveal the consequences for the existence and stability of equilibrium states in economic systems. An early contribution dealing with this problem can be found in Frisch and Holme (1935). Examples on more recent papers focusing on time delays in economic models are Keller (2010), Bianca et al. (2013), and Gori et al. (2018). In bioeconomics, several authors have analyzed the effects of absolute time delays both in single-population models and in predator–prey models (see, e.g., Bretschger & Smulders, 2018; Chakraborty et al., 2011, 2012; Ferrara et al., 2019; Gazi & Bandyopadhyay, 2008; Kar & Chakraborty, 2010; Martin & Ruan, 2001; Yuan et al., 2016; Q. Zhang et al., 2011; Y. Zhang et al., 2014). These papers show that the incorporation of absolute time delay effect results in a more complicated dynamics than what one obtains in standard population dynamical systems without delay. The incorporation of time delays in bioeconomic models is also found in more detailed discrete time simulations (see, e.g., Dolder et al., 2020; Gomes et al., 2021). Dolder et al. (2020) assume a given rate of delay when they simulate the fish population movement in space and time, whereas Gomes et al. (2021) assume an absolute time delay in the way temperature affects the biological efficiency for fish species. Notice that such absolute time delays are often motivated by specific biological mechanisms (e.g., gestation period or reaction time related to for instance reproductive or consumption behavior). The problem with absolute time delays is that in economic and biological systems it is not possible to give a precise estimate of the time lags, however. On the basis of this observation, it is argued that distributed time delay effects provide more realistic descriptions in economic-growth models. See, for example, Guerrini et al. (2020; and some of the references therein).

This serves as a motivation for the present study:

We analyze how a single species open-access commercial fishery is affected by marine pollution. Our model which is expressed in terms of a dynamical system is based on the simplifying assumption that production per capita in the economy grows with an exogenous given rate, and reaches an exogenous given saturation level in the long run. Furthermore, we assume that marine emissions are explained by means of this growth. Our objective is not to explain economic growth, but to analyze the possible consequences of economic growth for fisheries.

The modeling framework which we will present possesses a block structure: The solutions of the rate equations for the pollutant and the economic activity act as an input for the biomass and effort equation. This structure is reflected in the analysis of the existence and stability of the equilibrium states.

The proposed dynamical model deals with possible impacts of distributed time delays (instead of absolute time lags) on the fishery concerned. We incorporate these effects by expressing the pollutant level as a weighted decomposition of the instantaneous pollutant level and the corresponding time history of this level. The same type of decomposition applies to the economic activity state. We furthermore assume the weight functions in these delays to be modeled by means of exponentially decaying functions. This type of time delay modeling means that all earlier states matter, but the nearest history carries most weight. Similar ideas

concerning the ways time delays may influence the dynamics are found in Guerrini et al. (2020) analyzing economic growth. The assumption of exponentially decaying weight functions, enables us to convert the governing system of equations to a higher-order autonomous dynamical system by using the linear chain trick (LCT; Cushing, 2013). The resulting dynamical system is investigated with respect to existence and stability of equilibrium states. Moreover, using this conceptual way of treating time delays makes it possible to consider separation of time scales related to the different variables. More specifically, we expect the typical timescale for the biomass evolution to be much greater than the typical delay time scales for the pollutant and economic activity level. In this time-scale separation regime we show that the modeling framework becomes a singularly perturbed dynamical system. This system is analyzed by means of the Fenichel theory for singularly perturbed systems (Fenichel, 1979) and its generalization to multiple time scales (Cardin & Teixeira, 2017). We explore and illuminate important features of the modeling framework by means of the outcome of this asymptotic analysis and numerical simulations and show that the impact of the time history is negligible in the long run. Also here the block structure of the model plays an important role. As far as we know, this type of analysis has not been carried out for similar models earlier.

The present paper is organized as follows: In Section 2 we discuss our modeling framework in detail which is a modified version of Bergland et al. (2019). We transform the original system to a dimensionless system by means of scaling in Section 3 and introduce the aforementioned timescale separation regimes from the view point of bioeconomics. Section 4 is devoted to the analysis of the subsystem describing the economic-growth and pollution part of the model, whereas we carry out the analysis of the full model in Section 5. The analysis shows that the results obtained in Section 4 can be used as input in the full model presented in Section 5. Section 6 contains concluding remarks and a list of problems for future investigations. Appendix A contains the proof of the persistency property of the model. In Appendix B we deal with the application of the well-known Fenichel theory for one-parameter singularly perturbed dynamical systems to the economic-growth and pollution block of the modeling framework, whereas the same problem is addressed for the full modeling framework in Appendix C.

2 | MODELING FRAMEWORK

Our model consists of two main parts. One part models economic activity (production per capita) $Y(t)$ and stock of pollutant in the marine environment $S(t)$, whereas the other part describes a modified fishery model that constitutes the impact of pollution and economic growth on the fish stock $X(t)$ and dynamic effort variable $E(t)$. Without any time lag effects involved, the actual model reads

$$\begin{aligned} \frac{dX}{dt} &= rX\left(1-\frac{X+\beta S}{K}\right)-qXE, \quad \frac{dE}{dt}= k(qPX-c)E,\\ \frac{dS}{dt} &= \varrho_0 Y-\zeta\rho(S;a,b), \quad \frac{dY}{dt}= g(\bar{Y}-Y) \end{aligned} \tag{1}$$

with nonnegative initial conditions $X(0)>0, E(0)>0, S(0)>0, Y(0)>0$. The last two equations in the model (1) account for the assumption that production and consumption activities are responsible for the emission of harmful substances in the marine environment, and model the pollution absorptive capacity of the environment. The instantaneous change in

the production of pollution in the marine ecosystem is proportional to the production per capita Y with an emission rate ϱ_0. The nonmonotonic function ρ represents the remediation capacity function which is given as

$$\rho(S; a, b) = \frac{S + a}{S^2 + b^2}, \quad a, b > 0. \tag{2}$$

The remediation capacity function ρ which models the pollution absorptive capacity of the environment, thus depends on the size of the pollutant density. It constitutes a two-parameter family of functions parameterized by means of the remediation parameters a and b. Here the nonnegative function ρ is a twice differential function of S and has a global maximum value at a unique point $S = S_{\max} = \sqrt{a^2 + b^2} - a$. Here we notice that $\rho(S_{\max}; a, b) = 1/2S_{\max}$. Furthermore, ρ is a strictly increasing function for $0 \leq S \leq S_{\max}$ and strictly decreasing for $S \geq S_{\max}$. Notice that the function ρ also satisfies the homogeneity properties, that is,

$$\rho(S; a, b) = C\tilde{\rho}\left(\frac{S}{C}; \frac{a}{C}, \frac{b}{C}\right) \quad \text{for all real } C. \tag{3}$$

Hence, when the pollution level S is below the threshold value $S_{\max}$, the self-cleaning ability of the environment will increase with S. However, when exceeding this pollution threshold, the self-cleaning ability is expected to decrease and is negligible if pollution concentration in the marine ecosystem is high enough. A notable feature is that the remediation capacity function evaluated at $S_{\max}$ is inverse proportional to $S_{\max}$.

The last equation in the model (1) states that the change in production (and income) per capita is governed by the economic-growth function $f(Y; \bar{Y}) = \bar{Y} - Y$ and the economic-growth rate g, where the parameter $\bar{Y}$ is the unique zeros of the economic-growth function f. Moreover, $\lim_{t\to\infty} Y(t) = \bar{Y}$. Notice that the function f satisfies the homogeneity property, that is,

$$f(Y; \bar{Y}) = C\tilde{f}\left(\frac{Y}{C}; \frac{\bar{Y}}{C}\right) \quad \text{for all real } C, \tag{4}$$

where C is a positive parameter. It is worth mentioning that parameters $\bar{Y}$ and C have the same dimension.[1] The assumption of modeling an exogenous growth rate seems adequate as the production from the fishery only is assumed to contribute marginally to the total economic activity in the society. At the same time, we assume that emissions from fishing activities are insignificant compared with emissions from overall production and consumption in the economy.

For the other part of the model we assume a modified logistic growth equation for the development of the fish biomass with the negative term $-\beta S$ incorporated to account for the impact of pollution on the fish biomass. The parameter r measures the intrinsic growth rate of fish biomass and K is the carrying capacity. The coupling parameter β is referred to as the growth-retardation parameter. The model next considers the fish harvesting H where the fish supply from the harvesting follows the Gordon–Schaefer production function $H = qXE$. The instantaneous change in the effort variable E is assumed to be the proportion of the time-dependent sector profit $\pi = PH - cE$, where P is the time-dependent unit product fish price and c cost per unit price of fishing effort. The assumptions for the function P that represents the time-dependent marginal willingness to pay for fish products, include market demand–income–mechanisms and negative impact on fish demand due to pollution.

Inspired by the conjecture that the distributed delay framework appears to be more realistic and meaningful in the biological as well as in the economical context, we incorporate distributed time delays in the different modeling blocks of the model (1). First, we assume that the prehistory of the cleaning ability will affect the pollutant level S and should therefore be accounted for in the model extension. We take this property into account by making the replacement

$$\rho(S;a,b) \to p\rho(S;a,b) + (1-p)\rho(\langle S\rangle;a,b), \quad 0 \le p \le 1 \tag{5}$$

in the pollution equation of the model (1). Here $\langle S\rangle$ is the temporal mean defined as

$$\begin{aligned} \langle S\rangle(t) &\equiv \int_{-\infty}^{t} \alpha_\gamma(t-s)S(s)\,ds, \\ \alpha_\gamma(t) \ge 0, &\quad \int_0^\infty \alpha_\gamma(t)\,dt = 1. \end{aligned} \tag{6}$$

Thus, the new pollution equation which accounts for the prehistory of cleaning ability reads

$$\frac{dS}{dt} = \varrho_0 Y - \eta[p\rho(S;a,b) + (1-p)\rho(\langle S\rangle;a,b)]. \tag{7}$$

Next we take into account the impact of the distributed time delay in the saturation term of the fish biomass equation in (1). We do this by making the extension

$$\frac{dX}{dt} = rX\left(1 - \frac{X}{K} - \beta\frac{\omega S + (1-\omega)\langle S\rangle}{K}\right) - qXE, \quad 0 \le \omega \le 1, \tag{8}$$

of the biomass equation. Here the positive parameters r, K, and β have the same meaning as in (1). For a nonzero β the term $\beta\frac{\omega S + (1-\omega\langle S\rangle}{K}$ in (8) thus measures a possible loss in fish biomass depending upon the accumulated pollution and its corresponding past history. Notice that this term is a convex combination of the instantaneous effect of the pollution (modeled by means of S and the time history of the pollution development, represented by the mean value $\langle S\rangle$). The convexity parameter ω measures the degree of influence of the distributed time delay effect: For $\omega = 1$, no such effect is present, whereas for the other extreme case $\omega = 0$ the impact of the pollution effect on the wild fish population solely depends on the past history.

Regarding the price function P in the model (1), we assume that the price of the fish product is affected negatively by pollution and positively by economic activity (income per capita). The time-dependent marginal willingness to pay function P reads

$$P = P_1 + a_2(\kappa Y + (1-\kappa)\langle Y\rangle), \quad a_2 \ge 0, \;\; 0 \le \kappa \le 1. \tag{9}$$

Here $\langle Y\rangle$ is the temporal mean of the economic activity level Y defined as

$$\begin{aligned} \langle Y\rangle(t) &\equiv \int_{-\infty}^{t} \alpha_\mu(t-s)S(s)\,ds, \\ \alpha_\mu(t) \ge 0, &\quad \int_0^\infty \alpha_\mu(t)\,dt = 1. \end{aligned} \tag{10}$$

Moreover, we have assumed that the price function P depends on the pollutant density S and its corresponding time history $\langle S\rangle$, that is,

$$P_1 = A_0 - a_1 B_0(\nu F(S; B_0) + (1-\nu)F(\langle S\rangle; B_0)), \quad 0 \le \nu \le 1. \tag{11}$$

Here F is defined as

$$F(x; x_0) \equiv \frac{x}{x + x_0}$$

and

$$A_0 > 0, \quad B_0 \ge 0, \quad a_1 > 0.$$

We have imposed the constraint

$$a_1 B_0 \le A_0, \tag{12}$$

which ensures that the function P_1 is positive for all t. Thus we have assumed that distributed time lags are present in both the pollution level S and the income level Y in a way similar to the time lag effects in the biomass-pollution part of the modeling framework when it comes to the marginal willingness to pay function P.

The case $\nu = 1$ means that the effect of the past pollution history is negligible. To model P_1 we tacitly assume that accumulated pollution concentration affects the quality of the fish products and that it reduces the consumers beliefs in paying higher prices for the fish products. Therefore we assume that P_1 decreases for accumulating harmful substances in the marine ecosystem and it saturates to level $A_0 - a_1 B_0 > 0$. Here the positive constant A_0 measures a fixed market price for per capita income (Y). The nonnegative parameters a_1 and B_0 are responsible for modeling the consumers beliefs in the fish products. It promotes the willingness of consumers to pay less prices for such harmful fish products (Chen et al., 2015; Fonner & Sylvia, 2014; Garzon et al., 2016; Wessells & Anderson, 1995; Whitehead, 2006). Here we also assume that the history of pollution might affect the demand for fish, by incorporating a distributed time effect ($0 \le \nu < 1$).

With the assumption that the higher the income per capita, the higher aggregated demand for fish is, we model per capita economy production or the general income level per capita by mean of state variable Y. We model the positive influence of income level per capita Y on consumers demands for fish products that also includes a possible time delay income effect and an ordinary income impact on fish demand. By inserting the expression (9) for P into the rate equation for E in the model (1), we end up with the distributed time delay equation

$$\begin{aligned}\frac{dE}{dt} = k[&(A_0 - a_1 B_0(\nu F(S; B_0) + (1-\nu)F(\langle S\rangle; B_0)) \\ &+ a_2(\kappa Y + (1-\kappa)\langle Y\rangle))qX - c]E\end{aligned} \tag{13}$$

for the effort variable E. Regarding the temporal evolution of the economical activity level (production per capita), we retain the same rate equation as in the model (1), that is, we assume that

$$\frac{dY}{dt} = g(\bar{Y} - Y) \tag{14}$$

with an economic-growth rate g.

By making the additional assumption that the weight functions in the mean values $\langle S \rangle$ and $\langle Y \rangle$ defined by (6) and (10) are exponentially decaying functions, that is,

$$\alpha_\gamma(t) = \begin{cases} 0, & t < 0, \\ \gamma e^{-\gamma t}, & t \geq 0 \end{cases} \tag{15}$$

and

$$\alpha_\mu(t) = \begin{cases} 0, & t < 0, \\ \mu e^{-\mu t}, & t \geq 0, \end{cases} \tag{16}$$

the LCT produces the rate equations

$$\frac{d\langle S \rangle}{dt} = \gamma(S - \langle S \rangle) \tag{17}$$

and

$$\frac{d\langle Y \rangle}{dt} = \mu(Y - \langle Y \rangle) \tag{18}$$

for the mean values $\langle S \rangle$ and $\langle Y \rangle$. See Cushing (2013) for a detailed exposition on LCT.

To summarize, the modeling framework consists of the pollution dynamics equation (7), the fish biomass equation (8), the effort equation (13), and the production and income equation (14). The rate equation (17) for the mean value of the pollutant density and the rate equation (18) for the mean value of the economic activity level represent past history in the respective model variables. Thus our model comprises a 6D autonomous nonlinear dynamical system. The biological and/or economical interpretation of variables and the parameters of the proposed model are summarized in Table 1.

3 | GENERAL PROPERTIES OF THE MODEL

3.1 | Scaling and general properties of the model

We start out by observing that the exponentially decaying integral kernels α_γ and α_μ defined by (15) and (16) obey the scaling laws

$$\begin{aligned} &\alpha_{1/\varepsilon_\gamma}(\tau) = r^{-1}\alpha_\gamma(\tau r^{-1}), \quad \alpha_{1/\varepsilon_\mu}(\tau) = r^{-1}\alpha_\mu(\tau r^{-1}), \\ &\varepsilon_\gamma \equiv r\gamma^{-1}, \quad \varepsilon_\mu \equiv r\mu^{-1}, \\ &\alpha_d(t) = \begin{cases} 0, & t < 0, \\ de^{-dt}, & t \geq 0. \end{cases} \end{aligned} \tag{19}$$

TABLE 1 Interpretation of variables and parameters associated with the fishery-pollution models (8), (13), (7), and (14) and rate equations (17) and (18)

Variables/ parameters	Biological/ economical interpretation	Measurement units (dimensions)
t	Time	T
Y	Total production value per capita	C
S	The harmful substance density (stock of pollutants)	M
X	Fish population density	M
K	Carrying capacity of the fish biomass	M
H	Production volume (harvest) in fishery	$\mathrm{M\,T^{-1}}$
E	Effort (capital and labor) input in fishery	E
P	Market value of fish	$\mathrm{C\,M^{-1}}$
r	Intrinsic growth rate for the biomass	$\mathrm{T^{-1}}$
β	Pollution effect on biomass growth	1
q	Fixed harvest efficiency rate	$\mathrm{E^{-1}\,T^{-1}}$
g	Economy growth rate	$\mathrm{T^{-1}}$
$\bar{Y}$	Long-run production value per capita	C
$\wp_0$	Emission (pollution) rate	$\mathrm{MC^{-1}T^{-1}}$
ζ	Remediation (natural absorptive ability) rate	$\mathrm{T^{-1}}$
a	Remediation capacity parameter	M
b	Remediation capacity parameter	M
a_1	Pollution-demand impact fishery	$\mathrm{C\,M^{-2}\,T}$
a_2	Income-demand impact fishery	$\mathrm{M^{-1}}$
A_0	Potential fish price	$\mathrm{C\,M^{-1}}$
B_0	Price-saturation constant pollution	M
c	Cost per unit effort	$\mathrm{C\,E^{-1}T^{-1}}$
p	Weight of instantaneous versus delayed remediation capacity	1
ω	Weight of instantaneous versus delayed pollution effect on biomass growth	1
ν	Weight of instantaneous versus delayed market pollution effect	1
$\varkappa$	Weight of instantaneous versus delayed market income effect	1
k	Friction parameter in effort adjustment	$\mathrm{E\,C^{-1}}$

Note: The fundamental units are T for time (e.g., year, month), M for mass (e.g., tons, kg), E for effort (e.g., employee, capital), and C for currency (e.g., Euro, Yuan, etc.).

The scaled exponentially decaying kernels $\alpha_{1/\varepsilon_\gamma}$ and $\alpha_{1/\varepsilon_\mu}$ are normalized functions. Thus they can be used as weight functions in integrals that define the temporal means $\langle\theta\rangle$ and $\langle\psi\rangle$ of θ and ψ, respectively, that is,

$$\begin{aligned}\langle\theta\rangle(\tau) &\equiv \int_{-\infty}^{\tau} \alpha_{1/\varepsilon_\gamma}(\tau - s)\theta(s)\,ds,\\ \langle\psi\rangle(\tau) &\equiv \int_{-\infty}^{\tau} \alpha_{1/\varepsilon_\mu}(\tau - s)\psi(s)\,ds,\end{aligned} \tag{20}$$

where the functions $\langle\theta\rangle$ and $\langle\psi\rangle$ are defined in Table 2. Notice here that we can define $\langle\theta\rangle$ and $\langle\psi\rangle$ by means of (20) for any normalized integral kernels α_γ and α_μ that satisfy the scaling laws (19). We interpret the dimensionless parameters ε_γ and ε_μ: $T_\gamma = 1/\gamma$ is the decay time of the weight function α_γ in the temporal mean $\langle S\rangle$ of the pollutant density S, whereas $T_r = 1/r$ is the logistic timescale of the biomass X. Thus the ratio ε_γ is the ratio between these two time scales: $\varepsilon_\gamma = T_\gamma/T_r$. For ε_μ we get $\varepsilon_\mu = T_\mu/T_r$, where $T_\mu = 1/\mu$ is the decay time of the weight function α_μ in the temporal mean $\langle Y\rangle$ of the economical activity level Y. Thus ε_γ and ε_μ parametrize the temporal delay effects in our modeling framework. These two parameters (and consequently also the three timescales T_μ, T_γ, and T_r) will play a crucial role in the forthcoming analysis.

By means of the substitutions defined in Table 2 we readily derive the nondimensional version of the distributed delay system

$$\xi' = \xi\mathcal{F}(\xi,\eta,\theta,\psi,\langle\theta\rangle,\langle\psi\rangle), \qquad \eta' = \eta\mathcal{G}(\xi,\eta,\theta,\psi,\langle\theta\rangle,\langle\psi\rangle), \tag{21}$$

$$\theta' = \mathcal{H}(\xi,\eta,\theta,\psi,\langle\theta\rangle,\langle\psi\rangle), \quad \psi' = \mathcal{K}(\xi,\eta,\theta,\psi,\langle\theta\rangle,\langle\psi\rangle) \tag{22}$$

consisting of Equations (8), (7), (13), and (14). Here $\mathcal{F}$, $\mathcal{G}$, $\mathcal{H}$, and $\mathcal{K}$ are the functions defined as

$$\mathcal{F}(\xi,\eta,\theta,\psi,\langle\theta\rangle,\langle\psi\rangle) = 1 - \xi - \eta - \gamma_1(\omega\theta + (1-\omega)\langle\theta\rangle), \tag{23}$$

$$\begin{aligned}\mathcal{G}(\xi,\eta,\theta,\psi,\langle\theta\rangle,\langle\psi\rangle) = \gamma_6\xi - \gamma_7\xi\,[\nu F(\theta;\gamma_8) + (1-\nu)F(\langle\theta\rangle;\gamma_8)]\\ + \gamma_9\xi\,[\kappa\psi + (1-\kappa)\langle\psi\rangle] - \gamma_{10},\end{aligned} \tag{24}$$

$$\mathcal{H}(\xi,\eta,\theta,\psi,\langle\theta\rangle,\langle\psi\rangle) = \psi - \gamma_2[pR(\theta;\gamma_3) + (1-p)R(\langle\theta\rangle;\gamma_3)], \tag{25}$$

$$\mathcal{K}(\xi,\eta,\theta,\psi,\langle\theta\rangle,\langle\psi\rangle) = \gamma_4\tilde{f}(\psi;\gamma_5). \tag{26}$$

Here the notation $'$ means differentation with respect to the time variable τ. Table 2 summarizes the definitions and the interpretations of all the dimensionless variables and parameters involved in the nondimensionalization process of our modeling framework. Imposing the homogeneity assumptions (3) and (4) on the economic-growth function f and the remediation capacity ρ we get

$$f(\psi;\gamma_5) = C^{-1}\tilde{f}(C\psi;C\gamma_5), \quad C = \frac{ar}{\varrho}, \tag{27}$$

$$R(\theta,\gamma_3) \equiv \tilde{\rho}(\theta;1,\gamma_3) = a\rho(a\theta;a,b)). \tag{28}$$

The nondimensional version of economic-growth function f defined in (14) is obtained as

TABLE 2 Bioeconomic interpretation of the dimensionless variables τ, $\xi(\tau)$, $\eta(\tau)$, $\theta(\tau)$, $\langle\theta\rangle(\tau)$, $\psi(\tau)$, and $\langle\psi\rangle(\tau)$, and the parameters γ_i $(i = 1, 2, ..., 10)$, ι, ω, ε_γ, and ε_μ in the models (23)–(32)

Variable/parameter definition	Interpretation
$\tau = rt$	Dimensionless time (time t divided by the logistic time scale r^{-1})
$\xi(\tau) = X(t)/K$	Dimensionless fish stock population
$\eta(\tau) = qE(t)/r$	Dimensionless effort variable
$\theta(\tau) = S(t)/a$	Dimensionless pollution density
$\langle\theta\rangle(\tau) = \langle S\rangle(t)/a = \int_{-\infty}^{\tau} \alpha_{1/\varepsilon_\gamma}(\tau - s)\theta(s)\,ds$	Mean value of dimensionless pollution density
$\psi(\tau) = \wp_0 Y(t)/ra$	Dimensionless economic activity variable
$\langle\psi\rangle(\tau) = \wp_0\langle Y\rangle(t)/ra = \int_{-\infty}^{\tau} \alpha_{1/\varepsilon_\mu}(\tau - s)\theta(s)\,ds$	Mean value of dimensionless economic activity variable
$\gamma_1 = \beta a/K$	Biomass growth damage rate
$\gamma_2 = \zeta/ra^2$	Relative remediation rate
$\gamma_3 = b/a$	Remediation capacity parameter
$\gamma_4 = g/r$	Relative economic-growth rate
$\gamma_5 = \wp_0\bar{Y}/ra$	Relative long-run emission
$\gamma_6 = kqKA_0/r$	Potential revenue per unit effort in fishery
$\gamma_7 = ka_1B_0qK/r$	Pollution-demand impact
$\gamma_8 = B_0/a$	Demand parameter pollution
$\gamma_9 = kaqKa_2/\wp_0$	Income-demand impact
$\gamma_{10} = kc/r$	Relative unit cost of effort in fishery
$\iota = \gamma_5/\gamma_2$	Emission–remediation ratio
$\varepsilon_\gamma = r/\gamma$	Relative decay time of mean pollutant density $\langle S\rangle$
$\varepsilon_\mu = r/\mu$	Relative decay time of mean economical activity $\langle Y\rangle$

$$\tilde{f}(\psi; \gamma_5) = \gamma_5 - \psi. \tag{29}$$

Similarly when the remediation capacity function ρ is given as (2), we readily find that the *nondimensional remediation capacity* function R reads

$$R(\theta; \gamma_3) = \frac{\theta + 1}{\theta^2 + \gamma_3^2}. \tag{30}$$

The distributed delay systems (21)–(30) possess the following persistency property: If $\gamma_5 > \gamma_2[pR(0, \gamma_3) + (1 - p)R_{\max}]$, where $R_{\max} \equiv R(\theta_{\max}; \gamma_3)$ is the maximal value of the function $R(\theta; \gamma_3)$, $\theta \geq 0$, then any solution of the systems (21) and (22), which starts within the region

$$\Sigma = \{(\xi, \eta, \theta, \psi, \langle\theta\rangle, \langle\psi\rangle) : \xi > 0, \eta > 0, \theta > 0, \langle\theta\rangle > 0, \\ \psi > \gamma_2[pR(0, \gamma_3) + (1-p)R_{\max}], \langle\psi\rangle > 0\}, \tag{31}$$

remains in r for all $\tau \geq \tau^*$, where $\tau^* \leq 0$, that is, Σ is invariant under the solution flow of the systems (21) and (22). For the sake of completeness we have relegated the details of this proof to Appendix A (Theorem 1).

The mean values $\langle\theta\rangle$ and $\langle\psi\rangle$ given by (20) satisfy in accordance with the LCT the linear rate equations:

$$\varepsilon_\gamma \langle\theta\rangle' = \theta - \langle\theta\rangle, \quad \varepsilon_\mu \langle\psi\rangle' = \psi - \langle\psi\rangle \tag{32}$$

if the weight functions α_γ and α_μ are given as the exponentially decaying functions (15) and (16), respectively.

The dimensionless parameters γ_1, γ_2, γ_3, γ_4, γ_5, γ_6, γ_7, γ_8, γ_9, and γ_{10} associated with the modeling frameworks (21)–(32) are positive. Standard theory for dynamical systems guarantees that autonomous dynamical systems (21)–(32) are locally wellposed (Arnold, 1988; Guckenheimer & Holmes, 1983) and that any solution of the dynamical systems (21)–(32) will be a continuous function of the parameters $\gamma_1, ..., \gamma_{10}$. Furthermore, we classify model parameters into three groups based on their role in the dimensionless modeling framework:

- *Group* 1: Parameters influencing the economic-growth and pollution part of the dimensionless model: γ_2, γ_3, γ_4, and γ_5.
- *Group* 2: Parameters associated with economic growth and the pollution affecting the fishery part of the dimensionless model: γ_1, γ_7, γ_8, and γ_9.
- *Group* 3: Parameters affecting the fishery part of the dimensionless model: γ_6 and γ_{10}.

In the forthcoming analysis we refer to the parameter $\iota \equiv \frac{\gamma_5}{\gamma_2}$ as the *emission–remediation ratio*. By restoring to the original dimensional parameters we readily find that

$$\iota = \frac{\gamma_5}{\gamma_2} = \frac{\varrho_0 \bar{Y}}{\zeta a}. \tag{33}$$

Notice that the inequality (12) which is a sufficient condition for positive willingness to pay translates into the condition

$$\gamma_6 \geq \gamma_7. \tag{34}$$

We observe that the functions $\mathcal{H}$ and $\mathcal{K}$ defined by means of (25) and (26), respectively, are independent of ξ and η. This means that we can view the solutions of the subsystem

$$\begin{aligned} \theta' &= \mathcal{H}(\xi, \eta, \theta, \psi, \langle\theta\rangle, \langle\psi\rangle) = \psi - \gamma_2[pR(\theta; \gamma_3) + (1-p)R(\langle\theta\rangle; \gamma_3)], \\ \psi' &= \mathcal{K}(\xi, \eta, \theta, \psi, \langle\theta\rangle, \langle\psi\rangle) = \gamma_4 \tilde{f}(\psi; \gamma_5), \\ \varepsilon_\gamma \langle\theta\rangle' &= \mathcal{A}(\xi, \eta, \theta, \psi, \langle\theta\rangle) = \theta - \langle\theta\rangle, \varepsilon_\mu \langle\psi\rangle' = \mathcal{B}(\xi, \eta, \theta, \psi, \langle\theta\rangle) = \psi - \langle\psi\rangle \end{aligned} \tag{35}$$

as input functions to the subsystem

$$\xi' = \xi \mathcal{F}(\xi, \eta, \theta, \psi, \langle\theta\rangle, \langle\psi\rangle), \quad \eta' = \eta \mathcal{G}(\xi, \eta, \theta, \psi, \langle\theta\rangle, \langle\psi\rangle).$$

We further notice that the component functions $\mathcal{H}$, $\mathcal{K}$, and $\mathcal{A}$ in (35) are independent of the mean value $\langle\psi\rangle$. This means that the solution of the subsystem (35) can be determined by first obtaining the solution to the 3D system

$$\begin{aligned}\theta' &= \mathcal{H}(\xi,\eta,\theta,\psi,\langle\theta\rangle,\langle\psi\rangle) = \psi - \gamma_2[pR(\xi,\eta,\theta;\gamma_3) + (1-p)R(\langle\theta\rangle;\gamma_3)],\\ \psi' &= \mathcal{K}(\xi,\eta,\theta,\psi,\langle\theta\rangle,\langle\psi\rangle) = \gamma_4\tilde{f}(\psi;\gamma_5),\\ \varepsilon_\gamma\langle\theta\rangle' &= \mathcal{A}(\xi,\eta,\theta,\psi,\langle\theta\rangle,\langle\psi\rangle) = \theta - \langle\theta\rangle,\end{aligned} \tag{36}$$

and thereafter finding the temporal mean $\langle\psi\rangle$ by solving the linear rate equation

$$\varepsilon_\mu\langle\psi\rangle' = \mathcal{B}(\xi,\eta,\theta,\psi,\langle\theta\rangle,\langle\psi\rangle) = \psi - \langle\psi\rangle, \tag{37}$$

using ψ as an input function. Figure 1 summarizes schematically the relationship between the different blocks in the present model.

The asymptotic limit $\varepsilon_i \to 0^+$; $i = \gamma, \mu$ of the systems (21)–(30) is of particular interest from the viewpoint of bioeconomics: According to the previous discussion of the logistic timescale T_r and the delay time scales T_μ and T_μ, we observe that the parameter regime $0 < \varepsilon_i \ll 1$; $i = \gamma, \mu$ is equivalent with the time separation regime $T_\gamma \ll T_r$, $T_\mu \ll T_r$. This regime can be analyzed directly by means of the standard theory for singularly perturbed problems (Fenichel, 1979). If we impose the additional scale separation $\varepsilon_\mu/\varepsilon_\gamma = \gamma/\mu \ll 1 \Leftrightarrow T_\mu \ll T_\gamma$ (which can be motivated from viewpoint of bioeconomics), we end up with the two-parameter singularly perturbed system. Multiscale singularly perturbed dynamical systems can be dealt with using a generalization of Fenichel's theory (Cardin & Teixeira, 2017). In subsequent sections we will deal with these two parameter regimes.

4 | THE ECONOMIC-GROWTH AND THE POLLUTION PART OF THE MODEL

Here we discuss the properties of (35) and examine the impact of Group 1 parameters and delay weight parameter p on the dynamics of the subsystem (35). We start out by studying the existence of equilibrium points. An equilibrium point $\mathbb{E}_4 = (\theta_e, \psi_e, \langle\theta_e\rangle, \langle\psi_e\rangle)$ must satisfy

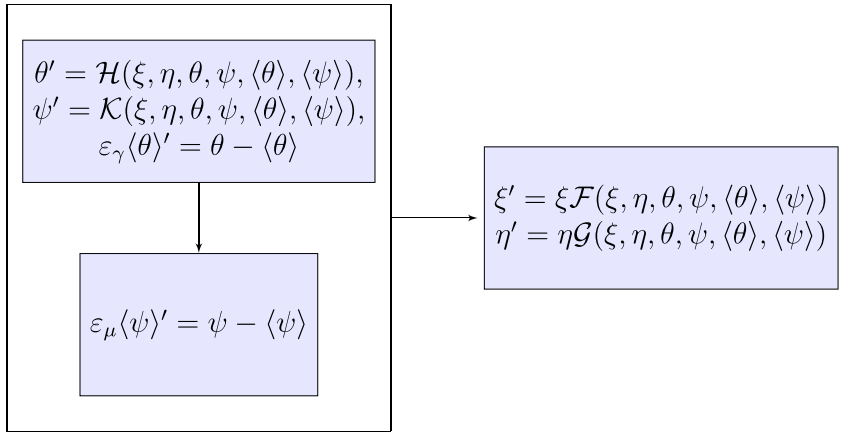

FIGURE 1 Schematic representation of the blocks in the models (21)–(30)

$\psi_e = \langle \psi_e \rangle = \gamma_5$ and $\langle \theta \rangle_e = \theta_e$ without any restriction. Hence the equilibrium problem boils down to a study of the equilibrium states (θ_e, γ_5) of the 2D system

$$\theta' = \psi - \gamma_2 R(\theta; \gamma_3), \quad \psi' = \gamma_4 \tilde{f}(\psi; \gamma_5). \tag{38}$$

We make use of the properties of this system when dealing with the study of the slow–fast regime $(0 < \varepsilon_i \ll 1)$ of (35) and (36). By utilizing the input parameters $\iota \equiv \frac{\gamma_5}{\gamma_2}$ and γ_3^2, the equilibrium condition boils down to the study of the equation

$$\frac{\theta + 1}{\theta^2 + \gamma_3^2} = \frac{\gamma_5}{\gamma_2}. \tag{39}$$

We denote the possible solutions of this equation as θ_e. Let us define a function $\Gamma : (0, \infty) \to (0, \infty)$ such that

$$\iota = \Gamma\left[\gamma_3^2\right] = \frac{1}{2} \frac{\sqrt{1 + \gamma_3^2} + 1}{\gamma_3^2}, \tag{40}$$

and introduce the subsets $\mathcal{Z}_{\text{non}}$, $\mathcal{Z}_{\text{eq},1}$, $\mathcal{Z}_{\text{eq},2}$, and $\mathcal{C}$ defined as

$$\begin{aligned} \mathcal{Z}_{\text{non}} &= \left\{ \left(\gamma_3^2, \iota\right) \in \mathbb{R}^2; \iota > \Gamma\left[\gamma_3^2\right] \right\}, \\ \mathcal{Z}_{\text{eq},2} &= \left\{ \left(\gamma_3^2, \iota\right) \in \mathbb{R}^2; \frac{1}{\gamma_3^2} < \iota < \Gamma\left[\gamma_3^2\right] \right\}, \\ \mathcal{Z}_{\text{eq},1} &= \left\{ \left(\gamma_3^2, \iota\right) \in \mathbb{R}^2; 0 < \iota \leq \Gamma\left[\gamma_3^2\right] \right\}, \\ \mathcal{C} &= \left\{ \left(\gamma_3^2, \iota\right) \in \mathbb{R}^2; \iota = \Gamma\left[\gamma_3^2\right] \right\}. \end{aligned} \tag{41}$$

Here the curve $\mathcal{C}$ represents the nontransversality condition $\iota = R\left(\theta_e; \gamma_3^2\right)$ and $R'\left(\theta_e; \gamma_3^2\right) = 0$. Notice that the region $\mathcal{Z}_{\text{non}}$ produces no equilibrium points whereas the parameter region $\mathcal{Z}_{\text{eq},2}$ produces exactly two equilibrium points. $\mathcal{Z}_{\text{eq},1}$ is the region which gives rise to one negative equilibrium point.

Now, let us assume that $\left(\gamma_3^2, \iota\right) \in \mathcal{Z}_{\text{eq},1} \cup \mathcal{Z}_{\text{eq},1} \cup \mathcal{C}$ which means that we are guaranteed the existence of at least one equilibrium point (and maximum two equilibrium points) of the type (θ_e, γ_5) of the 2D system (38). The stability problem of (38) can be resolved with the help of the Jacobian matrix

$$\mathbb{J}_2 = \begin{pmatrix} -\gamma_2 R'(\theta_e; \gamma_3) & 1 \\ 0 & -\gamma_4 \end{pmatrix}. \tag{42}$$

The eigenvalues of the above stability matrix are computed as $-\gamma_2 R'(\theta_e; \gamma_3)$ and $-\gamma_4$. Hence we conclude that the equilibrium point (θ_e, γ_5) is locally asymptotically stable if $R'(\theta_e; \gamma_3) > 0$ whereas it is saddle point if $R'(\theta_e; \gamma_3) < 0$. In the case $R'(\theta_e; \gamma_3) = 0$, the 2D subsystem (38) experiences a saddle-node bifurcation at the equilibrium point (θ_e, γ_5). For $R'(\theta_e; \gamma_3) = 0$, we

have a unique solution $\theta_e = \theta_{\max}$. Figure 2 shows a numerical example with the phase portrait of the 2D system (38) in the case when we have two equilibrium points, that is, $\left(\gamma_3^2, \iota\right) \in \mathcal{Z}_{\text{eq},2}$.

Let us assume $\left(\gamma_3^2, \iota\right) \in \mathcal{Z}_{\text{eq},2} \cup \mathcal{C}$ which means that we are in a regime for which the subsystem (36) has at least one positive equilibrium point $\mathbb{E}_3 = (\theta_e, \gamma_5, \theta_e)$, where θ_e satisfies (39). The Jacobian matrix for the 3D subsystem (36) at $\mathbb{E}_3$ is given as

$$\mathbb{J}_3^{(p)} = \left(\begin{array}{cc:c} \multicolumn{2}{c:}{\mathbb{J}_2^{(p)}} & \begin{matrix} -\gamma_2(1-p)R_e' \\ 0 \end{matrix} \\ \hdashline \frac{1}{\varepsilon_\gamma} & 0 & -\frac{1}{\varepsilon_\gamma} \end{array}\right). \tag{43}$$

where $\mathbb{J}_2(p)$ is the 2×2-block matrix given as

$$\mathbb{J}_2^{(p)} = \begin{pmatrix} -p\gamma_2 R'(\theta_e; \gamma_3) & 1 \\ 0 & -\gamma_4 \end{pmatrix}. \tag{44}$$

Here and in the sequel we will often make use of the abbreviation $R_e' \equiv R'(\theta_e; \gamma_3)$. The eigenvalues of (43) are given as

$$\begin{aligned} \lambda_\pm &= -\frac{1}{2\varepsilon_\gamma}[(1 + \gamma_2 pR'\varepsilon_\gamma) \pm \sqrt{(1 + \gamma_2 pR'\varepsilon_\gamma)^2 - 4R'\gamma_2\varepsilon_\gamma}], \\ \lambda_1 &= -\gamma_4 < 0. \end{aligned} \tag{45}$$

Thus the spectral properties of $\mathbb{J}_3^{(p)}$ show that equilibrium $\mathbb{E}_3$ is asymptotically stable if $R'(\theta_e; \gamma_3) > 0$ and a saddle point if $R'(\theta_e; \gamma_3) < 0$. The transition state $R'(\theta_e; \gamma_3) = 0$ corresponds

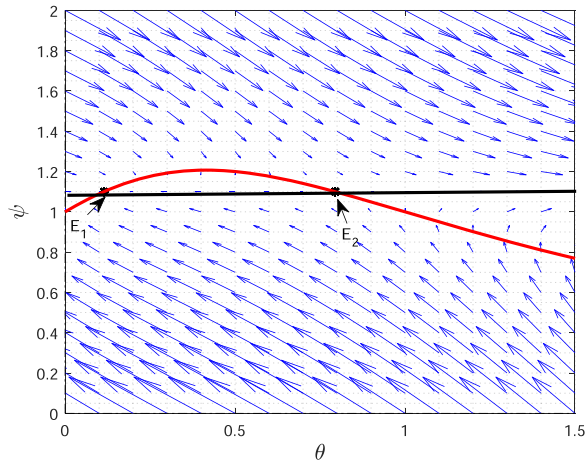

FIGURE 2 Nullclines of pollution θ (red curve), production variable ψ (black curve), and arrows showing the direction of the vector field to the system (38) for the input parameters $\gamma_2 = \gamma_3 = \gamma_4 = 1, \gamma_5 = 1.1, \iota = 1.1$. Here the equilibrium point $E_1 = (0.11, 1.1)$ (corresponding to $R'(\theta_e; \gamma_3) > 0$) is locally asymptotically stable and $E_2 = (0.78, 1.1)$ (corresponding to $R'(\theta_e; \gamma_3) < 0$) is a saddle point.

to a saddle-node bifurcation. This means that the weight parameter p does not change the stability properties as compared with the case $p = 1$. Thus the stability properties of the 2D subsystem (38) carry over to the 3D subsystem (36). We notice that $\mathbb{J}_2^{(p=1)} = \mathbb{J}_2$, where $\mathbb{J}_2$ is given by (42). The system (36) becomes a decoupled system in the case $p = 1$, in which the dynamical evolution of the state variables θ and ψ is governed by the 2D system (38), whereas the mean value $\langle\theta\rangle$ can be computed by solving the linear rate equation $\varepsilon_\gamma \langle\theta\rangle' = \theta - \langle\theta\rangle$ by direct integration treating θ as an input function obtained by solving (38).

Similarly, we linearize the 4D subsystem (35) around the equilibrium $\mathbb{E}_4$ to resolve the stability problem. One can easily compute the eigenvalues of the following Jacobian matrix to examine the stability of subsystem (35) at the equilibrium point $\mathbb{E}_4 = (\theta_e, \gamma_5, \theta_e, \gamma_5)$:

$$\mathbb{J}_4^{(p)} = \left(\begin{array}{ccc:c} & \mathbb{J}_3^{(p)} & & \begin{matrix}0\\0\\0\end{matrix} \\ \hdashline 0 & \frac{1}{\varepsilon_\mu} & 0 & -\frac{1}{\varepsilon_\mu} \end{array}\right). \tag{46}$$

Here we have tacitly assumed that the $\left(\gamma_3^2, \iota\right) \in \mathcal{Z}_{\text{eq},2} \cup \mathcal{C}$ which means that we are in a regime for which the subsystem (35) has at least one positive equilibrium state $\mathbb{E}_4$. Now by exploiting our findings for the Jacobian matrix $\mathbb{J}_3^{(p)}$ we can conclude that the weight parameter $p \in (0, 1)$ does not affect the stability of $\mathbb{E}_4$: The eigenvalues of $\mathbb{J}_4^{(p)}$ are given as

$$\begin{aligned} \lambda_\pm &= -\frac{1}{2\varepsilon_\gamma}[(1 + \gamma_2 pR'\varepsilon_\gamma) \pm \sqrt{(1 + \gamma_2 pR'\varepsilon_\gamma)^2 - 4R'\gamma_2\varepsilon_\gamma}\,, \\ \lambda_3 &= -\gamma_4 < 0, \quad \lambda_4 = -\frac{1}{\varepsilon_\mu} < 0 \end{aligned} \tag{47}$$

are strictly negative if the positive slope condition $R'(\theta_e; \gamma_3) > 0$ is satisfied whereas one of the eigenvalues is strictly positive if $R'(\theta_e; \gamma_3) < 0$. We also find that one eigenvalue becomes zero if $R'(\theta_e; \gamma_3) = 0$. Therefore the equilibrium $\mathbb{E}_4$ is locally asymptotically stable if $R'(\theta_e; \gamma_3) > 0$, whereas it will be a saddle point for the case $R'(\theta_e; \gamma_3) < 0$. Simple computation reveals that points located on the curve $\mathcal{C}$ correspond to a saddle-node bifurcation. It is worth noting that also in this case qualitative properties of the subsystem (35) follow the dynamical properties of the 2D subsystem (38).

In Figure 3 we present numerical results associated with a subsystem (35) which support the outcome of the present stability analysis. Here we have selected a set of parameter values $\gamma_2 = \gamma_3 = \gamma_4 = 1, p = 0.8, \gamma_5 = 1.1$ and depicted the dynamical evolution of the associated subsystem variables. In Figure 3a, we observe that the solution starting from the initial data $IC_1 = (0.6, 0.6, 0.3, 0.3)$ quickly converges to the equilibrium point $\mathbb{E}_{4,1} = (0.11, 1.1, 0.11, 1.1)$. However, the solution starting from initial data $IC_2 = (1.2, 0.6, 0.3, 0.3)$ gives rise to a saddle-node bifurcation that corresponds to an unstable equilibrium point $\mathbb{E}_{4,2} = (0.78, 1.1, 0.78, 1.1)$. Here we see that the dynamical variable ψ and its temporal mean $\langle\psi\rangle$ converge to the equilibrium value $\psi_e = 1.1$. However, the variable θ and its temporal mean $\langle\theta\rangle$ increase as time progresses (see Figure 3b). Obviously these findings are consistent with our theoretical outcomes. Here a moderate initial production per capita promotes stability. On the other hand, the accumulated pollution goes unbounded when the initial per capita production is high

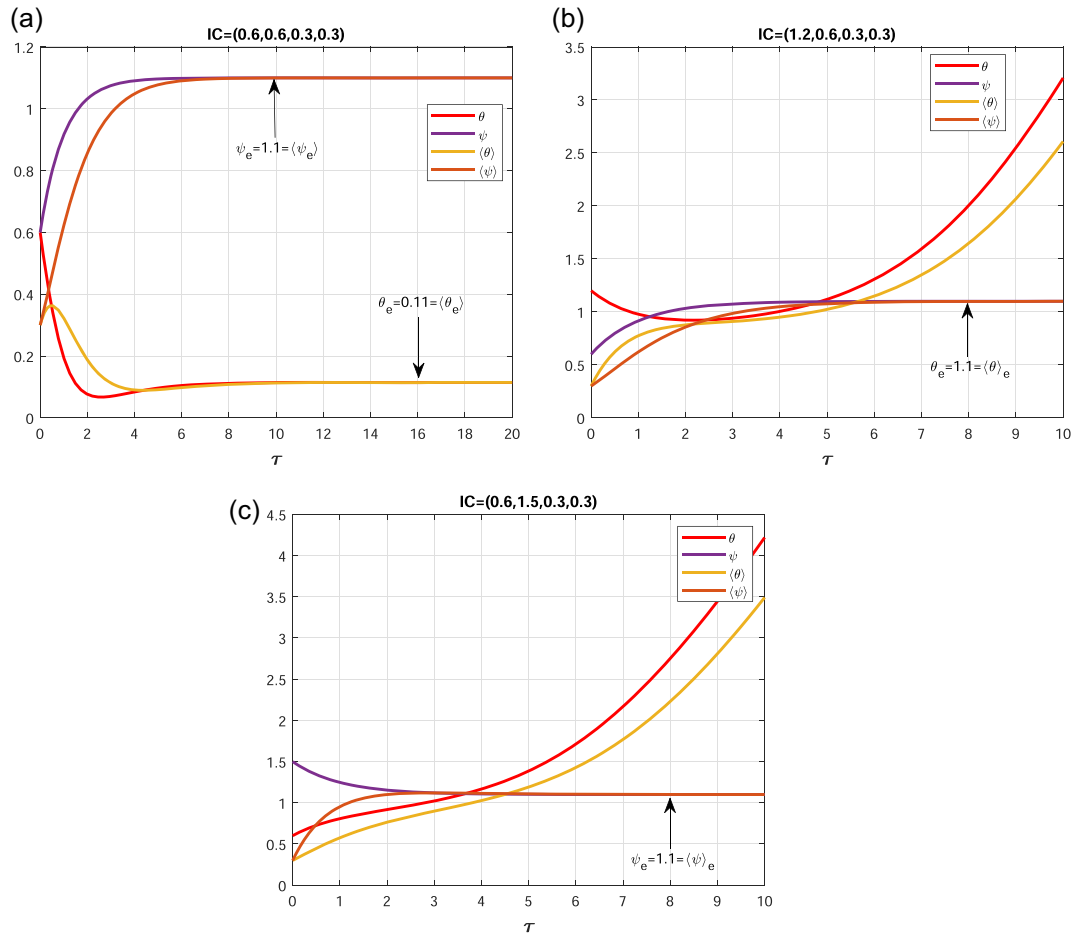

FIGURE 3 Numerical illustration of the subsystem (35) with $\varepsilon_\gamma = 1.0$. (a) Small perturbation (IC) in pollution θ (red curve) and economic activity ψ (violet curve) with its temporal mean converges to stable equilibrium $E_{\text{ep}} = (0.11, 1.1, 0.11, 1.1)$. (b) Uncontrolled pollution in case of high initial pollution. (c) Uncontrolled pollution in case of initially high economic activity.

enough. A similar situation is depicted in Figure 3c when initial production per capita exceeds a certain threshold.

4.1 | Slow–fast analysis

The subsystem (35) shows that the economic activity ψ and the pollution level θ do not depend on the past history of the economic activities. Therefore we will not include the equation of temporal mean $\langle\psi\rangle$ when studying the slow–fast progression analysis of the subsystem associated with the economic activity and the pollution part. A detailed mathematical analysis of a slow–fast version of the subsystems (35) and (36) is appended in Appendix B.

Here we show that numerical simulations of the dynamics of the slow–fast version of the subsystem (36) (i.e., the scaled subsystem B2) confirm the mathematical findings in Appendix B. This is illustrated in Figure 4. Here we have used $\gamma_2 = \gamma_3 = \gamma_4 = 1, p = 0.8, \varepsilon_\gamma = 0.01$, and

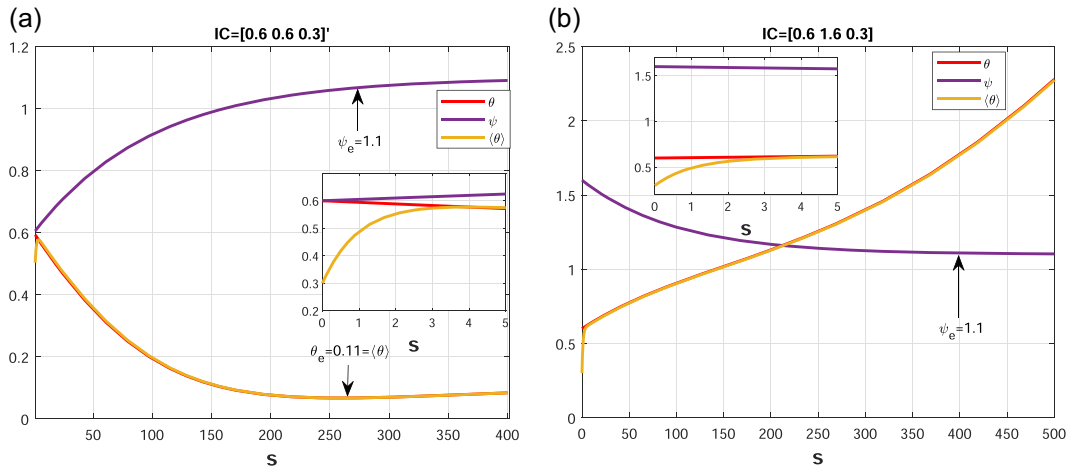

FIGURE 4 Numerical illustration of the subsystem (B2) with $\varepsilon_\gamma = 0.01$. (a) Small perturbation (IC) in the pollution θ (red curve), the economic activity ψ (violet curve) and pollution temporal mean $\langle\theta\rangle$ is attracting. (b) Uncontrolled pollution in case of initially high economic activity. Moreover, the economic activity ψ stabilizes as time progresses.

$\gamma_5 = 1.1$ as input parameters. The initial data used in the computations leading to Figure 4 is given as $(0.6, 0.6, 0.3)$. This simulation suggests that the variable $\langle\theta\rangle$ increases very fast following the dynamics of the layered problem until it reaches the attracting 2D equilibrium surface $\mathcal{M}^a$ defined by

$$\begin{aligned}\mathcal{M}^a &= \{(\theta, \psi, \langle\theta\rangle) \in \mathbb{R}^3 | \ \mathcal{A}(\xi, \eta, \theta, \psi, \langle\theta\rangle, \langle\psi\rangle) = 0\} \\ &= \{(\theta, \psi, \langle\theta\rangle) \in \mathbb{R}^3 | \ \langle\theta\rangle = \theta\}\end{aligned} \tag{48}$$

of $\mathbb{R}^3$. During this initial phase the variables θ and ψ stay almost constant. In the second phase they approach very slowly the asymptotically stable equilibrium on the slow manifold $\mathcal{M}^a$ as predicted by the reduced problem. In Figure 4b one can see that ψ (red curve) approaches its equilibrium value $\psi_e = 1.1$ slowly. Moreover, the mean value $\langle\theta\rangle$ (yellow curve) rapidly converges to θ (blue curve) following the dynamics of the fast subsystem on the slow-manifold $\mathcal{M}^a$. However, θ grows unbounded following the dynamics of the differential algebraic equation (DAE) problem. These numerical simulations suggest that a small singular parameter $0 < \varepsilon_\gamma \ll 1$ in (B2) does not destroy the qualitative properties of the subsystem (36).

From a bioeconomic point of view our analysis demonstrates that the bioeconomic time delay does not harm the stability of the slow–fast subsystem involving the pollution-economic part of the proposed model. Numerical simulations suggest that the mean variables $(\langle\theta\rangle, \langle\psi\rangle)$ are quickly attracted to equilibrium values (θ_e, ψ_e).

To conclude, we observe that the impact of the distributed time delay in the pollutant density and the economic activity is negligible in the long run in the time-scale separation regime $T_\mu, T_\gamma \ll T_r$, contrary to what is observed in models incorporating absolute time lags (Bretschger & Smulders, 2018; Chakraborty et al., 2011, 2012; Ferrara et al., 2019; Gazi & Bandyopadhyay, 2008; Kar & Chakraborty, 2010; Martin & Ruan, 2001; Yuan et al., 2016; Q. Zhang et al., 2011; Y. Zhang et al., 2014).

5 | ANALYSIS OF THE FULL SYSTEM

In this section we first discuss the existence and stability of equilibrium points of the full systems (21)–(30). If any such equilibrium points exist, then they must be in the form

$$(\xi, \eta, \theta, \psi, \langle\theta\rangle, \langle\psi\rangle) = (\xi_e, \eta_e, \theta_e, \gamma_5, \theta_e, \gamma_5), \tag{49}$$

where θ_e is a solution of Equation (39). This equation possesses no solutions if $\left(\iota, \gamma_3^2\right) \in \mathcal{Z}_{\text{non}}$ ($\iota \equiv \gamma_5/\gamma_2$), where $\mathcal{Z}_{\text{non}}$ is defined by means of (41). Therefore the original nondimensional systems (21)–(32) has no equilibrium states if $\left(\iota, \gamma_3^2\right) \in \mathcal{Z}_{\text{non}}$. In the complementary parameter regime, that is, when $\left(\iota, \gamma_3^2\right) \in \mathcal{Z}_{\text{eq},1} \cup \mathcal{Z}_{\text{eq},2} \cup \mathcal{C}$, Equation (39) has at least one solution and maximum two solutions. This means that $\left(\iota, \gamma_3^2\right) \in \mathcal{Z}_{\text{eq},1} \cup \mathcal{Z}_{\text{eq},2} \cup \mathcal{C}$ is a necessary condition for the systems (21)–(32) to have equilibrium states. We keep this condition in mind during the upcoming analysis of the proposed model.

In Section 5.1 we study the possibility of having equilibrium points of the system located in the hyperplanes $\xi = 0$ and $\eta = 0$ with the corresponding stability properties, whereas we in Section 5.2 deal with conditions ensuring the existence of equilibrium points in the first orthant. In the latter subsection we address the stability of the interior equilibrium points. The stability assessment of the equilibrium points (49) is inferred from the spectral properties of the Jacobian matrix. We also illustrate the theoretical findings by means of numerical simulations in these subsections.

5.1 | Existence and stability of equilibrium points in the hyperplanes $\xi = 0$ and $\eta = 0$

The equilibrium problem consists of investigating solutions of the system

$$\xi_e \mathcal{F}(\xi_e, \eta_e, \theta_e, \gamma_5, \theta_e, \gamma_5) = 0, \quad \eta_e \mathcal{G}(\xi_e, \eta_e, \theta_e, \gamma_5, \theta_e, \gamma_5) = 0,$$

where the functions $\mathcal{F}$ and $\mathcal{G}$ are defined by means of (23) and (24), respectively.

Assume that $\xi_e = 0$. We readily find that $\mathcal{G}(0, \eta_e, \theta_e, \gamma_5, \theta_e, \gamma_5) = -\gamma_{10} < 0$ from which it follows that the only possibility for having an equilibrium point in this case is that $\eta_e = 0$. Hence the equilibrium point in the hyperplane $\xi = 0$ is

$$Q_0 = (0, 0, \theta_e, \gamma_5, \theta_e, \gamma_5). \tag{50}$$

For the purpose of investigating the stability of Q_0, we first derive the Jacobian $\mathbb{J}_6$ evaluated at Q_0. Simple computation reveals that

$$\mathbb{J}_6(Q_0) = \left(\begin{array}{cc:c} 1 - \gamma_1\theta_e & 0 & 0_{2\times 4} \\ 0 & -\gamma_{10} & \\ \hdashline 0_{4\times 2} & & \mathbb{J}_4^{(p)} \end{array}\right). \tag{51}$$

where $0_{m\times n}$ denotes the zero $m \times n$ matrix. The eigenvalues of the Jacobian matrix (51) are given by means of (47) and

$$\lambda_5 = 1 - \gamma_1\theta_e, \quad \lambda_6 = -\gamma_{10} < 0 \tag{52}$$

from which we arrive the following conclusions: If $\theta_e < \gamma_1^{-1}$, then the equilibrium point Q_0 is unstable, regardless of the sign of the slope parameter $R'(\theta_e; \gamma_3)$. In the complementary regime $\theta_e > \gamma_1^{-1}$, Q_0 will be asymptotically stable if $R'(\theta_e; \gamma_3) > 0$ and a saddle point if $R'(\theta_e; \gamma_3) < 0$. The transition states $\theta_e = \gamma^{-1}$ and $R'(\theta_e; \gamma_3) = 0$ represent bifurcation points for which the stability assessment cannot be based on the linearization procedure.

In Figure 5, we numerically illustrate the stability of the equilibrium point Q_0 and try to examine how the pollution and the economic activity part affect the fishery dynamics. Here we observe that for a certain set of parameter values and initially low pollution density, the economic activities and the pollution level are sustained and remain in the vicinity of their respective equilibrium values (θ_e, ψ_e). We also observe the eradication of the fish biomass together with a vanishing of the harvesting effort consistent with the stability properties of the equilibrium point Q_0. In the case the pollution goes uncontrolled we notice a rapid extinction of the fish population and the vanishing of the harvesting effort (see Figure 5b).

Let us next consider the hyperplane $\eta = 0$. In this case we either get $\xi_e = 1 - \gamma_1\theta_e$ or $\xi_e = 0$. The former value of ξ_e produces the equilibrium point

$$Q_1 = (1 - \gamma_1\theta_e, 0, \theta_e, \gamma_5, \theta_e, \gamma_5). \tag{53}$$

To get a positive ξ_e we must impose the restriction $\gamma_1\theta_e < 1$. It is important to notice that $Q_0 = Q_1$ if $\gamma_1\theta_e = 1$. Let us consider the regime $R(0; \gamma_3) < \frac{\gamma_5}{\gamma_2} < R(\theta_{\max}; \gamma_3)$ (corresponding to $\left(\iota, \gamma_3^2\right) \in \mathcal{Z}_{\text{eq},2}$) for which we have two positive solutions of Equation (39), $\theta_e = \theta_l$ and $\theta_e = \theta_h$ $(\theta_l < \theta_h)$ corresponding to $R'(\theta_l; \gamma_3) > 0$ and $R'(\theta_h; \gamma_3) < 0$, respectively. Notice that if $\gamma_1\theta_h \le 1$, we will have $\gamma_1\theta_l \le 1$ Thus we will have the coexistence of two equilibrium points of the type Q_1 for the case $\gamma_1\theta_h \le 1$ and $\theta_l < \theta_h$.

We next compute the Jacobian $\mathbb{J}_6$ evaluated at Q_1:

$$\mathbb{J}_6(Q_1) = \left(\begin{array}{cc:c} -\xi_e & -\xi_e & \mathbb{A}_1 \\ 0 & \mathcal{G}(Q_1) & \\ \hdashline & 0_{4\times 2} & \mathbb{J}_4^{(p)} \end{array}\right) \tag{54}$$

Here

$$\mathbb{A}_1 = \begin{pmatrix} -\gamma_1\omega\xi_e & 0 & -\gamma_1(1-\omega)\xi_e & 0 \\ 0 & 0 & 0 & 0 \end{pmatrix}$$

and

$$\mathcal{G}(Q_1) = \xi_e(\gamma_6 + \gamma_5\gamma_9 - \gamma_7 F(\theta_e; \gamma_8)) - \gamma_{10}$$

and ξ_e is defined in (53). The eigenvalues of the stability matrix (54) are given by (47) and

$$\lambda_3 = -(1 - \gamma_1\theta_e) < 0, \quad \lambda_4 = \mathcal{G}(Q_1).$$

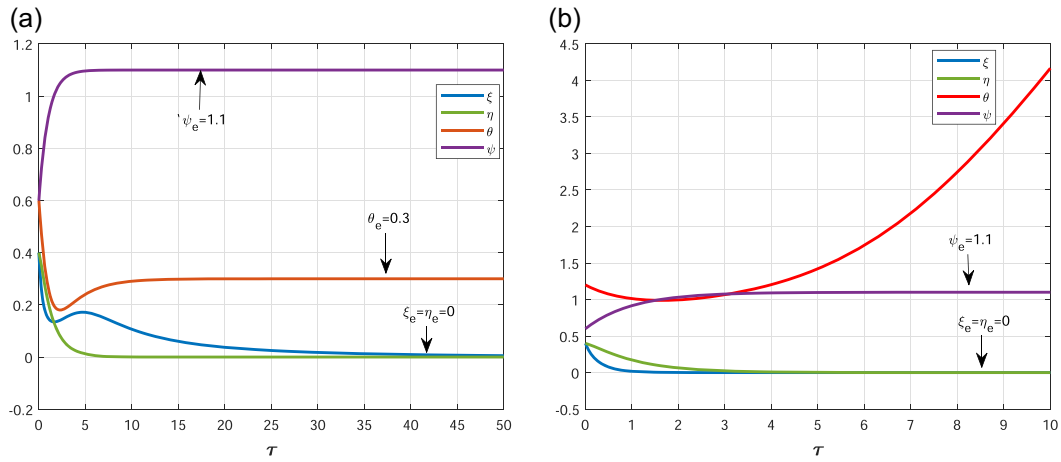

FIGURE 5 Dynamical behavior of nondimensional systems (21)–(32) in the vicinity of the equilibrium point Q_0 in the high biomass damage regime. Input parameters: $\gamma_1 = 3.5, \gamma_2 = \gamma_3 = 1.1, \gamma_4 = 1, \gamma_5 = 1.1, \gamma_6 = 2, \gamma_7 = 1, \gamma_8 = 0.5, \gamma_9 = 0.1, \gamma_{10} = 1, \varepsilon_\gamma = \varepsilon_\mu = 1$. (a) Initial condition $(0.4, 0.4, 0.6, 0.6, 0.6, 0.6)$ belongs to the attractor basin of Q_0. The fishery sector is wiped out and the effort vanishes. (b) Initial condition $(0.4, 0.4, 1.2, 0.6, 0.6, 0.6)$ does not belong to the attractor basin of Q_0. The fish stock is depleted very quickly and the pollution grows uncontrolled due to high initial pollution production. Here ξ represents fish biomass, η is the effort variable, θ measures the concentration of pollution, and ψ is the economic activity.

Following the spectral properties of submatrix $\mathbb{J}_4^p$ we are in the position to claim that Q_1 is an asymptotically stable equilibrium if $R'(\theta_e; \gamma_3) > 0$ and $\mathcal{G}(Q_1) < 0$. The latter condition is equivalent with the restriction

$$0 < \xi_e < \frac{\gamma_{10}}{\gamma_6 + \gamma_5\gamma_9\kappa - \gamma_7 F(\theta_e; \gamma_8)} \tag{55}$$

imposed on ξ_e since by (59) in Remark 1 the condition

$$\gamma_6 + \gamma_5\gamma_9\kappa - \gamma_7 F(\theta_e; \gamma_8) > 0$$

always is fulfilled.

Figure 6 demonstrates the impact of the pollution on the stability properties of the equilibrium point Q_1. In Figure 6a we observe that a small perturbation around Q_1 does not harm its stability. Notice that this long-run evolution of the pollution level makes the fishery unprofitable, thus resulting in a vanishing of the effort even though the fish stock has not gone extinct. However, Figure 6b shows that an initially high pollution level also causes the extinction of the fish biomass. This means that the solution is attracted towards the equilibrium Q_0.

5.2 | Existence and stability of positive equilibrium points

Here we discuss the existence and stability of positive equilibrium points, that is, equilibrium points of the type (49) for which $\xi_e, \eta_e, \theta_e > 0$. By using the equilibrium condition

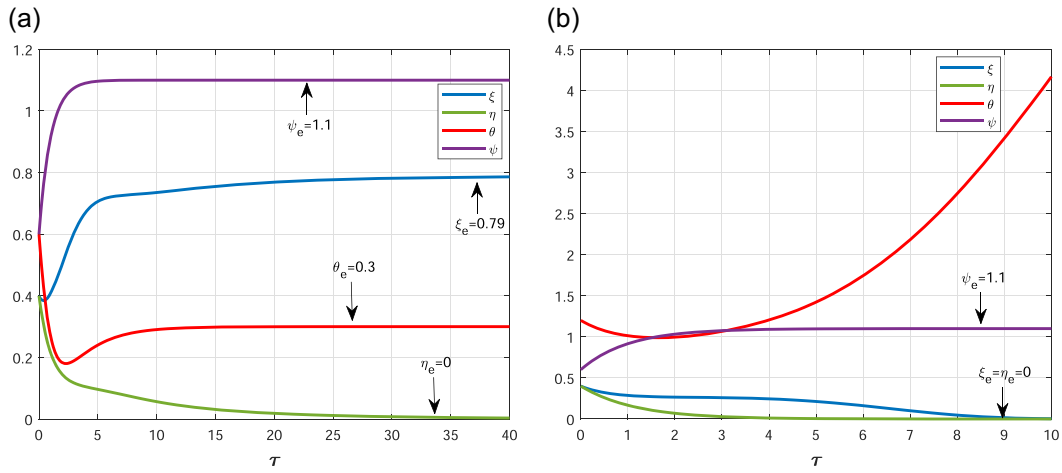

FIGURE 6 Dynamical behavior of nondimensional systems (21)–(32) in the vicinity of the equilibrium point Q_1 in the high pollution-demand impact regime. Input data: $\gamma_7 = 2.5$, $\gamma_1 = 3.5$, $\gamma_2 = \gamma_3 = 1.1$, $\gamma_4 = 1$, $\gamma_5 = 1.1$, $\gamma_6 = 2$, $\gamma_8 = 0.5$, $\gamma_9 = 0.1$, $\gamma_{10} = 1$, $\varepsilon_\gamma = \varepsilon_\mu = 1$. (a) Initial condition $(0.4, 0.4, 0.6, 0.6, 0.6, 0.6)$ (moderate initial pollution level) belongs to the attractor basin of Q_1. The fish stock ξ is sustainable, whereas the economic effort η vanishes. (b) Initial condition $(0.4, 0.4, 1.2, 0.6, 0.6, 0.6)$ does not belong to the attractor basin of Q_1. The fish stock ξ is depleted very quickly, the effort vanishes η, and the pollution θ level grows uncontrolled due to the high initial pollution level.

$$\mathcal{F} = 1 - \xi_e - \eta_e - \gamma_1\theta_e = 0, \quad \mathcal{G} = \gamma_6\xi_e - \gamma_7\xi_e F(\theta_e;\gamma_8) + \gamma_9\xi_e\psi_e - \gamma_{10} = 0,$$

we express ξ_e and η_e in terms of θ_e:

$$\eta_e = 1 - \xi_e - \gamma_1\theta_e, \quad \xi_e = \frac{\gamma_{10}}{\gamma_6 + \gamma_5\gamma_9 - \gamma_7 F(\theta_e;\gamma_8)}. \tag{56}$$

According to Remark 1 the restrictions

$$0 < \xi_e < 1 - \gamma_1\theta_e, \quad \gamma_6 + \gamma_5\gamma_9 - \gamma_7 F(\theta_e;\gamma_8) > 0 \tag{57}$$

will always be fulfilled. This means that we are guaranteed the existence of positive equilibrium points Q_e provided the subsystem (36) has at least one positive equilibrium point.

Remark 1. We notice that the first inequality in (57) is equivalent to the boundedness condition

$$X_e + \beta S_e < K \tag{58}$$

for the equilibrium biomass X_e and the equilibrium pollutant density S_e (corresponding to ξ_e and θ_e, respectively) when restoring to the dimensional parameters. The result (58) shows that X_e is bounded by the carrying capacity K whereas S_e is bounded by K/β. The second inequality in (57) is the nondimensional version of the positive marginal willingness to pay, that is, the condition,

$$P_e = A_0 + a_2\bar{Y} - a_1 B_0 \frac{S_e}{S_e + B_0} > 0. \tag{59}$$

By restoring to the dimensional parameters, we find that the equilibrium effort E_e and the equilibrium population density X_e (corresponding to Equation 56) are given as

$$E_e = \frac{r}{q}\left[1 - \frac{c}{qKP_e} - \frac{\beta}{K}S_e\right], \quad X_e = \frac{c}{qP_e}. \tag{60}$$

Here P_e is the marginal willingness to pay given as (59), also interpreted as the market value per unit catch. We notice that the equilibrium biomass X_e and the equilibrium fishery effort E_e are determined by fish value, cost, harvest efficiency, and growth parameters in a similar manner as in the standard Gordon–Schaefer model (e.g., Clark, 2010; Flaaten, 2018; Hannesson, 1978). For instance, it follows that the special case with no biomass growth damage ($\beta = 0$) our equilibrium (corresponding to the effort and stock level) is referred to as the bioeconomic equilibrium of the unregulated open-access fishery in the standard Gordon–Schaefer model. The cost–value ratio ($\frac{c}{P_e}$) is crucial when determining the profitability in the fishery, and thereby the equilibrium biomass and the equilibrium fishery effort. If $X > X_e$, fishing is profitable and the effort increases causing a reduction of the biomass. As soon as X falls below X_e, fishing becomes unprofitable and the effort will be withdrawn.

Now to determine the stability of the positive equilibrium point Q_e we first derive the Jacobian matrix $\mathbb{J}_6$ evaluated at this point. We readily obtain

$$\mathbb{J}_6(Q_e) = \left(\begin{array}{cc:c} -\xi_e & -\xi_e & \\ \mathcal{G}_\xi(Q_e) & 0 & \mathbb{A}_e \\ \hdashline 0_{4\times 2} & & \mathbb{J}_4^{(p)} \end{array}\right) \tag{61}$$

where

$$\mathbb{A}_e = \begin{pmatrix} -\gamma_1\omega\xi_e & 0 & -\gamma_1(1-\omega)\xi_e & 0 \\ -\gamma_7\xi_e\nu F'(\theta_e;\gamma_8) & \gamma_9\kappa\xi_e\eta_e & -\gamma_7\xi_e(1-\nu)F'(\theta_e;\gamma_8) & \gamma_9(1-\kappa)\xi_e\eta_e \end{pmatrix}$$

and

$$\mathcal{G}_\xi(Q_e) = \gamma_6 + \gamma_5\gamma_9 - \gamma_7 F(\theta_e;\gamma_8). \tag{62}$$

The eigenvalues of stability matrix (61) are given by

$$\lambda_\pm^e = -\frac{1}{2}[\xi_e \pm \sqrt{\xi_e(\xi_e - 4\mathcal{G}_\xi(Q_e)}] \tag{63}$$

and those eigenvalues which can be extracted from submatrix $\mathbb{J}_4^{(p)}$, that is, the expressions (47). From Remark 1 we know that $\mathcal{G}_\xi(Q_e) > 0$ (see condition 57). We observe that eigenvalues $\lambda_\pm^e$

remain negative if the condition $\xi_e > 4\mathcal{G}_\xi(Q_e)$ is satisfied. Combining this condition with (57) we get the following restriction:

$$F(\theta_e; \gamma_8) > \frac{1}{\gamma_7}\left(\gamma_6 + \gamma_5\gamma_9 - \frac{\sqrt{\gamma_{10}}}{2}\right), \tag{64}$$

which ensures negative values of $\lambda_{\pm}^{e}$. Here the structure of the function $F(\theta_e; \gamma_8)$ is defined in (12). Remark 2 gives a detailed bioeconomic interpretation of the condition (64). It is noteworthy that the condition (64) is interlinked with the stability dynamics of the fisheries and economic effort part which are automatically satisfied if the condition (57) is satisfied. Assuming that the condition (64) is fulfilled, the stability assessment of the positive equilibrium point Q_e simplifies the study of the slope of the remediation capacity R evaluated at θ_e: Q_e is a locally asymptotically stable equilibrium if the positive slope condition $R'(\theta_e; \gamma_3) > 0$ holds true. A saddle-node bifurcation occurs when $R'(\theta_e; \gamma_3) = 0$. Q_e becomes unstable if $R'(\theta_e; \gamma_3) < 0$. We illustrate this result numerically. To this end, we run simulations for a set of parameters satisfying the restrictions stated in (56) which ensure the positivity of the equilibrium point Q_e. In Figure 7, one can easily see how an initially high pollutant level may alter the dynamics of a stable equilibrium point. In Figure 7a, we observe that a small disturbance of the equilibrium point Q_e does not harm the stability of the system. However, an initially high pollutant density promotes uncontrolled pollution which may harm the stability of the system. It is worth mentioning that a high initial pollution level may give rise to the bifurcation from the interior equilibrium point Q_e to the fisheries-effort eradication equilibrium point Q_0 (see Figure 7a).

We also signify the effect of Group 3 parameters on the stability of the interior equilibrium point Q_e. We numerically observe that Group 3 parameters have no impact on the equilibrium value of the state variables θ, ψ. Therefore we only capture the time evolution of state variables ξ and η in the upcoming simulations.

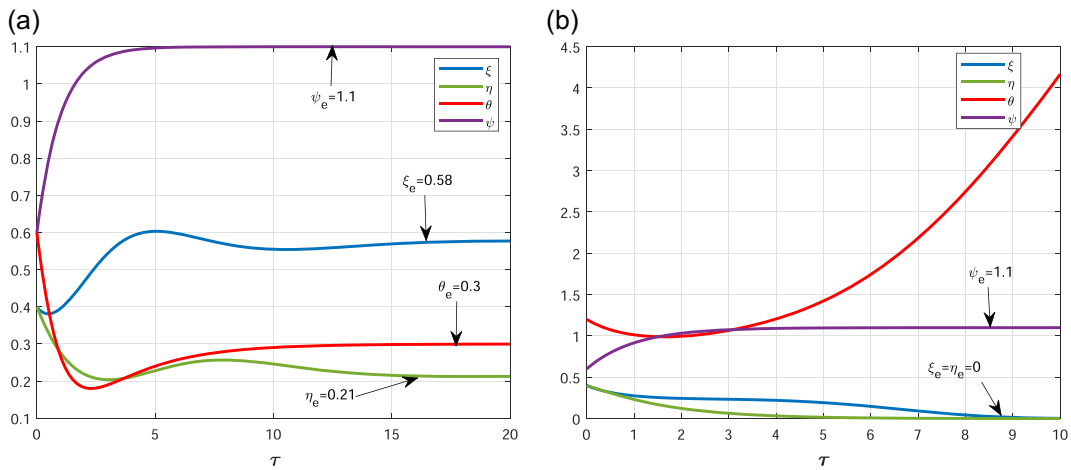

FIGURE 7 Dynamical behavior of nondimensional systems (21)–(32) in the vicinity of the equilibrium point Q_e. Parameter values are $\gamma_1 = 0.7, \gamma_2 = \gamma_3 = 1.1, \gamma_4 = 1, \gamma_5 = 1.1, \gamma_6 = 2, \gamma_7 = 1, \gamma_8 = 0.5, \gamma_9 = 0.1, \gamma_{10} = 1, \varepsilon_\gamma = \varepsilon_\mu = 1$. (a) Initial condition (0.4, 0.4, 0.6, 0.6, 0.8, 0.8) representing a moderate initial pollution level belongs to the attractor basin of Q_e. The fish stock ξ and economic effort η are sustained and remain stable for the small perturbation. (b) The initial condition (0.4, 0.4, 1.2, 0.6, 0.8, 0.8) representing a high initial pollution level results in rapid extinction of the fish stock ξ and a vanishing economic effort η, whereas the pollution level θ grows unbounded.

Remark 2. By restoring to the dimensional parameters, we find that the inequality (64) translates into the boundedness condition

$$P_e < \frac{1}{2qK}\sqrt{\frac{rc}{k}}. \tag{65}$$

Here P_e is the marginal willingness to pay defined by means of (59). We notice the appearance of the market value per unit, in addition to the harvest efficiency (q), the growth parameters (r and K), and the friction in effort adjustment (k) in this expression. We conclude from the above analysis that the equilibrium Q_e is asymptotically stable as long as the market value P_e in the fishery is below this threshold level and for small and moderate values of the equilibrium pollutant level.

5.3 | Slow–fast analysis

In this subsection we apply geometrical singular perturbation theory to investigate the dynamics of slow–fast progression in the original system. We discuss different cases depending on the values of parameters μ and γ.

5.3.1 | Case I: $T_\mu \sim T_\gamma \ll T_r$

This subsection is devoted to study the slow–fast progression dynamics of the systems (21)–(32) under the time-scale separation $T_\mu \sim T_\gamma \ll T_r$. This regime can be investigated by means of Fenichel's theory (Fenichel, 1979) and its generalization to multitime-scale problems (Cardin & Teixeira, 2017) for slow–fast systems. The application of this theory to our model is relegated to Appendix C.

Here we focus on how the numerical simulation matches the theoretical findings presented in Appendix C. To this end we consider the flow of the slow part of the system (35) (i.e., the subsystem C1) on the 4D critical manifold $\mathcal{M}_0$ defined by

$$\mathcal{M}_0 = \{(\xi, \eta, \theta, \psi, \langle\theta\rangle, \langle\psi\rangle) \in \mathcal{R}^6 : \langle\theta\rangle = \theta, \langle\psi\rangle = \psi\}. \tag{66}$$

This evolution is governed by the system

$$\begin{aligned} \xi' &= \xi(1 - \xi - \eta - \gamma_1\theta), \quad \eta' = \eta(\gamma_6\xi - \gamma_7\xi F(\theta; \gamma_8) + \gamma_9\xi\psi - \gamma_{10}), \\ \theta' &= \psi - \gamma_2 R(\theta; \gamma_3), \quad \psi' = \gamma_4\tilde{f}(\psi; \gamma_5). \end{aligned} \tag{67}$$

Here we see that the economic activity variable ψ evolves independently of the remaining state variables as time progresses. Moreover it is always attracted to its equilibrium $\psi_e = \gamma_5$. We recall the results obtained in previous sections to determine the stability of equilibrium points of the system (67): If $\theta_e = \theta_l$ be the solution of (39) for which $R'(\theta_e, \gamma_3) > 0$, then the interior equilibrium $\mathcal{E}_l = (\xi_e, \eta_e, \theta_l, \gamma_5)$ of the system (67) is locally asymptotically stable whereas the other equilibrium point $\mathcal{E}_h = (\xi_e, \eta_e, \theta_h, \gamma_5)$ corresponding to the negative slope condition $R'(\theta_e, \gamma_3) < 0$ is unstable within the framework of the model (67). Notice that this stability result is independent of ε_γ. The mathematical analysis carried out in Appendix C suggests that

the impact of distributed delay over the long period of time is negligible in the time-scale regime $T_\mu \sim T_\gamma \ll T_r$.

To illustrate the mathematical observations appended in Appendix C we run numerical simulations for the same set of parameter values and initial data underlying the computations leading to Figure 7. We observe a rapid attraction of fast variables $\langle\theta\rangle$ and $\langle\psi\rangle$ towards their equilibrium points. The slow variables evolve very slowly and almost look like constant in this phase (see Figure 8).

In Figure 9, we present numerical results for the regime $0 < \varepsilon_\mu = \varepsilon_\gamma \ll 1$ showing the temporal evolution of the biomass ξ and the effort variable η by assuming the

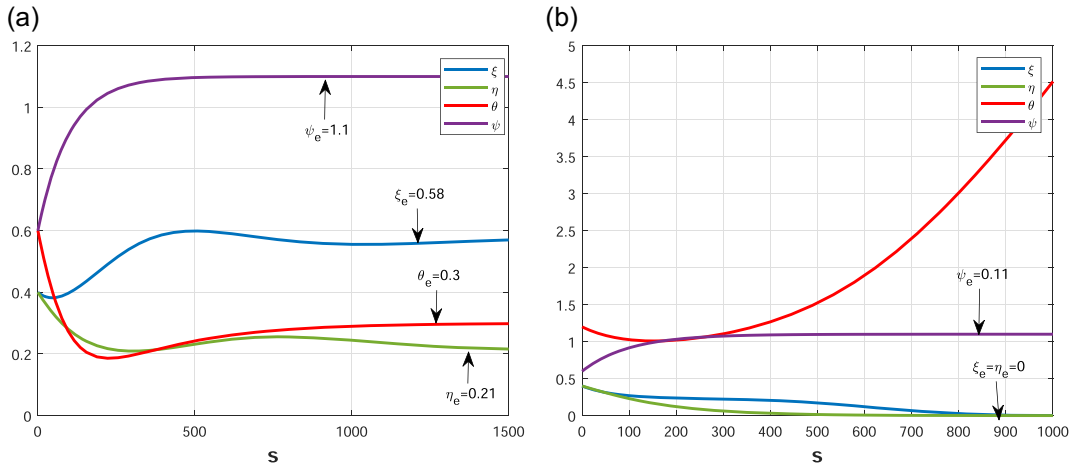

FIGURE 8 Temporal evolution of slow variables of the singularly perturbed system (67). Parameter values (except $\varepsilon_\gamma = \varepsilon_\mu = 0.01$) and initial data are the same as in Figure 7a,b. Here ξ represents fish biomass, η is the effort variable, θ measures the concentration of pollution, and ψ is the economic activity.

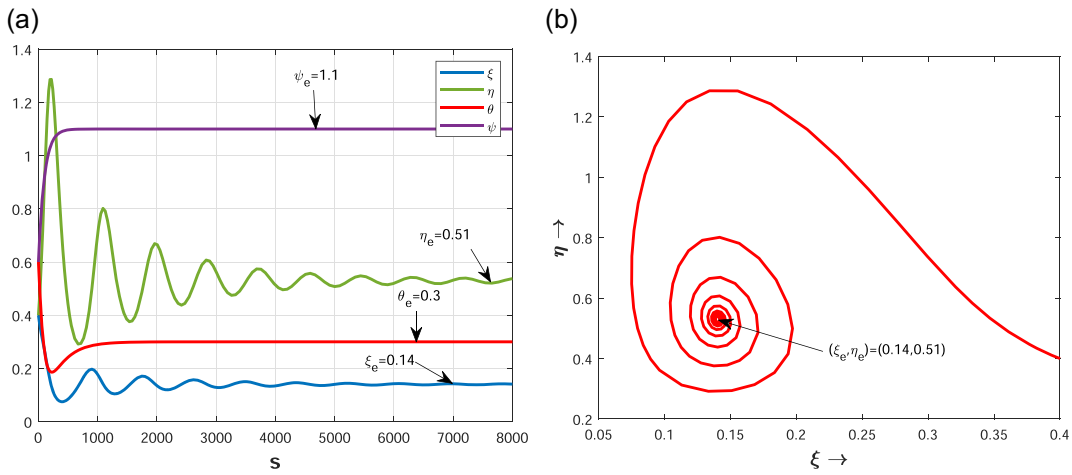

FIGURE 9 Temporal evolution of slow variables of the reduced system (67) on the critical manifold $\mathcal{M}_\varepsilon$. Parameter values are $\gamma_1 = 1.1, \gamma_2 = \gamma_3 = 1.1, \gamma_4 = 1, \gamma_5 = 1.1, \gamma_6 = 2, \gamma_7 = 1, \gamma_8 = 0.5, \gamma_9 = 5, \gamma_{10} = 1, \varepsilon_\gamma = \varepsilon_\mu = 0.01$. The initial condition is the same as in Figure 7a. Here ξ represents fish biomass, η is the effort variable, θ measures the concentration of pollution, and ψ is the economic activity.

pollution-economic activity block as input information to the fishery part. In Figure 9a we observe the well-known oscillations where the profitability in the fishery determines the effort, and the following harvest volume causes biomass variations. Figure 9 displays the temporal evolution of the slow variable which is evolved on slow manifold $\mathcal{M}_{\varepsilon_\gamma}$. These simulations demonstrate how a general trajectory of the system (67) is attracted towards the slow manifold.

5.3.2 | Case II: $T_\mu \ll T_\gamma \ll T_r$

Finally, we study the dynamics of the full systems (21)–(32) in the time-scale separation regime $T_\mu \ll T_\gamma \ll T_r$. This means that $\varepsilon_\mu \ll \varepsilon_\gamma (\Leftrightarrow r \ll \gamma \ll \mu)$. We use the slow–fast analysis carried out in Section 4.1 to conclude that the dynamical evolution decomposed into the three phases described in that subsection: In the first phase the temporal mean variable associated with economic activity, $\langle\psi\rangle$, evolves on the fastest time scale T_μ, with the remaining variables $(\xi, \eta, \theta, \psi, \langle\theta\rangle)$ being constant. The 5D subspace

$$\mathcal{M}_1 = \{(\xi, \eta, \theta, \psi, \langle\theta\rangle, \langle\psi\rangle) \in \mathbb{R}^6 : \langle\psi\rangle = \psi\}$$

of $\mathbb{R}^6$ acts as a normally attracting hyperbolic manifold. The dynamical evolution in the next phase takes place on $\mathcal{M}_1$ and is governed by the system

$$\begin{aligned} \xi' &= \xi\mathcal{F}(\xi, \eta, \theta, \psi, \langle\theta\rangle, \langle\psi\rangle), \quad \eta' = \eta\mathcal{G}(\xi, \eta, \theta, \psi, \langle\theta\rangle, \langle\psi\rangle), \\ \theta' &= \mathcal{H}(\xi, \eta, \theta, \psi, \langle\theta\rangle, \langle\psi\rangle), \quad \psi' = \mathcal{K}(\xi, \eta, \theta, \psi, \langle\theta\rangle, \langle\psi\rangle), \\ \varepsilon_\gamma \langle\theta\rangle' &= \theta - \langle\theta\rangle, \end{aligned} \tag{68}$$

which is a singularly perturbed system with ε_γ as a perturbation parameter. As $\varepsilon_\gamma \to 0$, the asymptotic approximation of the dynamical evolution prescribed by (68) decomposes into two phases: The first phase consists of the evolution of the mean value of the pollution on the intermediate time scale T_γ with the remaining variables $(\xi, \eta, \theta, \psi)$ being constant and the 4D subspace

$$\mathcal{M}_2 = \{(\xi, \eta, \theta, \psi, \langle\theta\rangle, \langle\psi\rangle) \in \mathbb{R}^6 : \langle\theta\rangle = \theta, \langle\psi\rangle = \psi\}$$

of $\mathcal{M}_1$ acting as a normally attracting hyperbolic manifold. The final phase consists of the slow evolution of $\mathcal{S} = (\xi, \eta, \theta, \psi)$ on the manifold $\mathcal{M}_2$. The 4D autonomous governing system (67) acts as the reduced problem on $\mathcal{M}_2$ for the slow dynamical systems (21)–(30) which is already discussed in the previous sections. Now we consider following transformations:

$$\begin{aligned} &\tilde{\tau} = \tau/\varepsilon_\gamma, \quad \varsigma(\tilde{\tau}) = \xi(\tau), \quad \Phi(\tilde{\tau}) = \eta(\tau), \quad \chi(\tilde{\tau}) = \theta(\tau), \\ &\Psi(\tilde{\tau}) = \psi(\tau), \quad \langle\chi\rangle(\tilde{\tau}) = \langle\theta\rangle(\tau), \quad \langle\Psi\rangle(\tilde{\tau}) = \langle\psi\rangle(\tau), \end{aligned}$$

and letting $\varepsilon_\gamma = 0$ in dynamical systems (21)–(30) we get the intermediate problem on $\mathcal{M}_1$

$$\tilde{\varsigma} = 0, \quad \tilde{\Phi} = 0, \quad \tilde{\chi} = 0, \quad \tilde{\varphi} = 0, \quad \tilde{\langle\chi\rangle} = \chi - \langle\chi\rangle,$$

where ~ denotes the time derivative with respect to the intermediate time variable $\tilde{\tau}$. The other variables remain constant on this time scale. Similarly, the associated layered problem is given by

$$\dot{\Lambda} = 0, \quad \dot{\Upsilon} = 0, \quad \dot{\Theta} = 0, \dot{\Psi} = 0, \quad \langle \dot{\Theta} \rangle = 0, \quad \langle \dot{\Psi} \rangle = \Psi - \langle \Psi \rangle.$$

Here $\dot{\cdot}$ denotes the time derivative with respect to $\hat{\tau}$ where time variable $\hat{\tau} = \tilde{\tau}/\varepsilon_\mu$ and other state variables are transformed similarly as in (B1). Notice that $\mathcal{M}_1$ and $\mathcal{M}_2$ are the critical and two-critical manifolds on which the intermediate and the reduced problems of systems (21)–(30) are defined, respectively. Notice that $\mathcal{M}_1$ and $\mathcal{M}_2$ are also the equilibrium points of the layered and the intermediate problem of the systems (21)–(30). By appealing to Theorems A, B, C, and Corollary 1 in Cardin and Teixeira (2017) we conclude that for small parameters ε_μ and ε_γ, there is an invariant manifold $\mathcal{M}_2^{(\varepsilon_\mu,\varepsilon_\gamma)}$ under the flow of the systems (21)–(30) which is the perturbed counterparts of the manifold $\mathcal{M}_2$ with Hausdorff distance $\mathcal{O}(\varepsilon_\mu + \varepsilon_\gamma)$ and, it is diffeomorphic to $\mathcal{M}_2$. Moreover, the stability property of $\mathcal{M}_2^{(\varepsilon_\mu,\varepsilon_\gamma)}$ is inherited from the attracting critical manifold $\mathcal{M}_2$. We omit the proof of multitime-scale convergence results for the slow–fast systems as these results follow directly from Theorems A, B, and C in Cardin and Teixeira (2017).

We finally run simulations for the singularly perturbed original systems (21)–(30) in the parameter regime $0 < \varepsilon_\mu < \varepsilon_\gamma \ll 1$. The outcome of these simulations is summarized in Figure 10. Here we observe that the mean variables $\langle\theta\rangle$ and $\langle\psi\rangle$ converge to the trajectories of θ and ψ very quickly, respectively. However, the slow variables evolve very slowly on the same time interval in comparison. These variables remain almost constant in the initial phase (see magnified view in Figure 10a). However, in the long run the slow variables converge to their respective equilibrium values. The numerical findings thus agree surprisingly well with the predictions deduced by means of the theory for singularly perturbed systems, even though $\varepsilon_\gamma = 5\varepsilon_\mu$ in the numerical simulations. We conclude that neither the past history of economic activities nor the past history of pollution growth will affect the fishery dynamics in the long run in this time separation regime. Moreover, high initial pollution level gives rise to uncontrolled pollution growth which in turn promotes unprofitable fisheries and could be the reason for the extinction of the fish biomass.

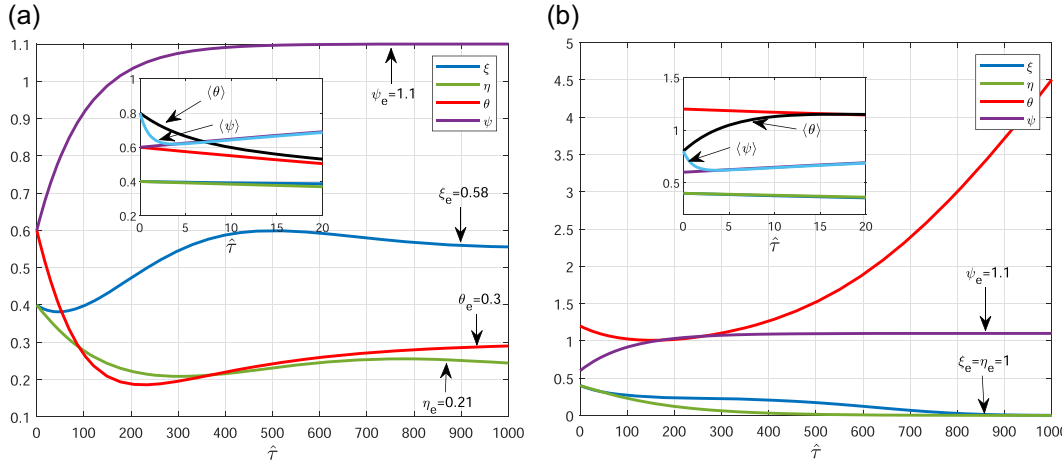

FIGURE 10 Temporal evolution of slow variables of the singularly perturbed systems (21)–(30). The parameter values (except $\varepsilon_\gamma = 0.05$, $\varepsilon_\mu = 0.01$) and the initial data are the same as in Figure 7a,b. Here ξ represents the fish biomass, η is the effort variable, θ measures the concentration of pollution, ψ is the economic activity, and $\hat{\tau}$ is the time scale for the equivalent fast system of the original models (21)–(30).

6 | CONCLUDING REMARKS AND EXTENSIONS

6.1 | Main results

In the present paper we have investigated a conceptual causal bioeconomic model describing the impact of pollution on a fishery using a dynamical system approach. We have accounted for distributed time histories in both the pollution level and the economic activity level in this modeling framework. This means that the fundamental model assumes the form of a distributed time delay system. The model decomposes into two subsystems. The first subsystem which describes the interaction between the pollution and the economic activity plays the role as an input to the second subsystem which is defined as rate equations for the fish stock density and the effort variables.

The model is converted to a 6D autonomous dynamical system by means of the LCT when assuming the weight functions in the time delay terms to be exponentially decaying functions (Cushing, 2013). Existence and stability of equilibrium states are investigated. We also identify the characteristic time scales for these time lags and investigate the dynamical evolution as a function of these time scales. When the former time scales are much smaller than the logistic time scale, the modeling framework becomes a singularly perturbed dynamical system. We have analyzed this system using Fenichel's theory (Fenichel, 1979) and its generalization to multiscale problems (Cardin & Teixeira, 2017) together with numerical simulations. On the basis of this analysis and the simulation results we conclude that the prominent feature to be observed is that the impact of the distributed time lags is negligible in the long-run dynamical evolution, contrary to what is found for population dynamical systems with absolute time lags (Bretschger & Smulders, 2018; Chakraborty et al., 2011, 2012; Ferrara et al., 2019; Gazi & Bandyopadhyay, 2008; Kar & Chakraborty, 2010; Martin & Ruan, 2001; Yuan et al., 2016; Q. Zhang et al., 2011; Y. Zhang et al., 2014). Hence, our model analysis adds to the existing literature knowledge of how distributed time delays affect short- and long-run development of stock and effort in an open-access harvesting model.

6.2 | Possible extensions

Here we will point to possible extensions and modifications of the present modeling framework which could be topics for future research.

First, in the present paper we have assumed that the emission rate ϱ_0 in the pollution equation is constant, compare Equation (7). A natural extension of this assumption consists of modeling the emission rate by means of a strictly decreasing, which is bounded from above and below. The motivation for assuming a decrease in the emission rate as a function of the pollutant density and the economic activity goes as follows: First, when the production increases (which implies a higher income in the economy), it seems reasonable to expect that the individuals' preferences for reducing the pollution become relatively more important. If such reasoning holds, the environmental policies will become stricter. Second, an increase in emissions may also lead to an increased willingness to implement stricter environmental standards to avoid the negative impacts from pollution. However, it is reasonable to believe that the emission rate remains positive and saturates when assuming such decreasing effects.

Second, we have assumed the time histories to be modeled by means of exponentially decaying functions. We have argued that this assumption mimics a realistic time history when

it comes to economic activity and pollution emission. We do not exclude the possibility that other time histories can be relevant, however. One possible future research topic consists of assuming that the time histories can be modeled as a Taylor - polynomial multiplied with an exponentially decaying function. This type of time history can model situations where certain times in the past carry more weights than others when it comes to the influence of the time history on the present situation. The LCT is applicable in this case. See Cushing (2013). It will produce a higher hierarchy of ordinary differential equations (ODEs). Here a detailed numerical examination of the change in the temporal development of the state variables would be of interest. One should, however, be aware of that the change to this type of weight function will not alter the fundamental stability properties of the detected equilibrium states. Notice also that the time-scale separation regimes which also in this case can be analyzed by means of Fenichel's theory for singularly perturbed dynamical systems (and its extension to multiscale problems) will also lead to the conclusion that the impact of the delay effects on the dynamical evolution will be negligible in the long run.

The argument for this proceeds in the same way as in Sections 4 and 5. Notice that it is possible to extend the LCT method to generally distributed time lags as suggested in Ponosov et al. (2004). However, in this case LCT may produce an infinite dimensional system of ODEs, so that it may be a mathematical challenge to perform stability analysis, and there is no guarantee that the properties of the present model would be preserved under such a far-reaching generalization. However, if the lag distribution is polynomial-based, the LCT gives a finite-dimensional system, and the stability analysis can be performed in the standard way, as explained above.

Third, a natural and well-motivated extension consists of incorporating spatial effects in the modeling framework. This means to consider effects like local as well as nonlocal advection–diffusion effects in the description of the biomass evolution as well as in the pollutant movement. We believe that such spatial effects are not present in the rate equations for the economic activity and the effort variables. Here we could follow the same line of thought as in Marciniak-Czochra et al. (2017) and Heilmann et al. (2018). This means that the modeling framework assumes the form of an ODE–reaction diffusion coupled model with advection effects incorporated. The key problem here will be to detect linear instabilities of equilibrium states as a route to pattern formation. The outcome of this process is expected to be stationary spatial patterns, standing, and traveling waves, and possibly also chaotic spatiotemporal patterns. It will thus be of interest to find out if the resulting system permits coherent structures like stable traveling wave solutions. The role of such structures in the pattern-forming process should be examined. Here we should notice that nonlocal diffusion effects incorporated in the biomass and the pollutant equation in a way analogous to Cheng and Yuan (2017) could result in the existence of traveling waves. Another interesting problem for further investigation is to study the proposed model under biomass diffusion as an optimal fisheries management problem. The main idea is to investigate the effects of optimal control of biomass diffusion processes in the emergence of spatial heterogeneity through diffusion-driven instability. Optimal control in harvesting and diffusion in the emergence of spatial heterogeneity can be studied based on the footprints of William and Xepapadeas (2010).

Fourth, we will expect that the determination of the maximal remediation capacity as well as other parameters will be subject to uncertainties, and thus the stochastic processes should be included in the modeling framework. Hence the modeling framework becomes a system of stochastic differential equations. Following the thoughts as in Evans (2012) and

Øksendal (2003), the model can be rewritten as an autonomous dynamical system of first-order equations with the stochastic effects accounting for additive noise terms in the system.

In addition to more sophisticated and realistic assumptions regarding the pollution and the cleaning abilities of the ecosystem, alternative and more reasonable assumptions regarding the economic behavior and the functioning of the fish market also represent possible model extensions. For instance, modifications of Verhulst's population growth model and the Gordon–Schaefer harvest production function which are discussed in Hannesson (1978), Clark (2010), Flaaten (2018), or Eide (2018), could be incorporated in the model formulation.

Seeking for an overall welfare optimal resource allocation, environmental, and fishery policies based on the predictions derived from a model like ours would also be an interesting task for future research.

To sum up, our comments regarding possible extensions may serve as a relevant background for future studies concerning marine pollution and fishery resources within the framework of bioeconomic models.

AUTHOR CONTRIBUTIONS

Harald Bergland: Conceptualization (equal), formal analysis (equal), methodology (equal), writing—original draft (equal), and writing—review and editing (equal). **Purnedu Mishra**: Conceptualization (equal), formal analysis (equal), methodology (equal), writing—original draft (equal), and writing—review and editing (equal). **Pål Andreas Pedersen**: Conceptualization (equal), formal analysis (equal), methodology (equal), writing—original draft (equal), and writing—review and editing (equal). **Arkadi Ponossov**: Conceptualization (equal), formal analysis (equal), methodology (equal), writing—original draft (equal), and writing—review and editing (equal). **John Wyller**: Conceptualization (equal), formal analysis (equal), methodology (equal), writing—original draft (equal), and writing—review and editing (equal). All of the authors have the equal contribution.

ACKNOWLEDGMENTS

The present work was initiated in Spring 2021. The authors are grateful to Professor Ola Flåten and Professor Arne Eide (The Arctic University of Norway) for fruitful and stimulating discussions during the preparation phase of this paper. The authors would also like to thank the reviewers and the editor for constructive remarks. This research work was supported by the Norwegian University of Life Sciences and The Research Council of Norway, project number 239070.

CONFLICT OF INTEREST

The authors declare no conflict of interest.

ORCID

Harald Bergland http://orcid.org/0000-0002-8913-7577
Purnedu Mishra http://orcid.org/0000-0001-8585-255X
Pål Andreas Pedersen http://orcid.org/0000-0003-0092-2518

ENDNOTE

[1] This specification means the existence of a unique long-run saturation level for the production per capita given by $\bar{Y}$, which can be interpreted as the equilibrium state in output per worker in accordance with the

Solow growth model (Solow, 1956). Our model does not explicitly include factors affecting the level of economic growth.

REFERENCES

Arnold, V. I. (1988). *Geometrical methods in the theory of ordinary differential equations*. Springer Verlag.

Bergland, H., Burlakov, E., Pedersen, P. A., & Wyller, J. (2020). Aquaculture, pollution and fishery-dynamics of marine industrial interactions. *Ecological Complexity*, *43*, 100853.

Bergland, H., Pedersen, P. A., & Wyller, J. (2019). Accumulated marine pollution and fishery dynamics. *Ecological Complexity*, *38*, 56–74.

Bianca, C., Ferrara, M., & Guerrini, L. (2013). The time delays' effects on the qualitative behavior of an economic growth model. In *Abstract and applied analysis* (Vol. 2013).

Bretschger, L., & Smulders, S. (2018). Taking time for the environment: On timing and the role of delays in environmental and resource economics. *Environmental and Resource Economics*, *70*(4), 731–736.

Cardin, P. T., & Teixeira, M. A. (2017). Fenichel theory for multiple time scale singular perturbation problems. *SIAM Journal on Applied Dynamical Systems*, *16*(3), 1425–1452.

Chakraborty, K., Chakraborty, M., & Kar, T. (2011). Bifurcation and control of a bioeconomic model of a prey–predator system with a time delay. *Nonlinear Analysis: Hybrid Systems*, *5*(4), 613–625.

Chakraborty, K., Jana, S., & Kar, T. (2012). Effort dynamics of a delay-induced prey–predator system with reserve. *Nonlinear Dynamics*, *70*(3), 1805–1829.

Chen, X., Alfnes, F., & Rickertsen, K. (2015). Consumer preferences, ecolabels, and effects of negative environmental information. *AgBioForum*, *18*(3), 327–336.

Cheng, H., & Yuan, R. (2017). Existence and stability of traveling waves for Leslie–Gower predator–prey system with nonlocal diffusion. *Discrete & Continuous Dynamical Systems*, *37*, 5433.

Chevé, M. (2000). Irreversibility of pollution accumulation. *Environmental and Resource Economics*, *16*(1), 93–104.

Clark, C. (2010). *Mathematical bioeconomics. The mathematics of conservation*. John Wiley and Sons Inc.

Cushing, J. M. (2013). *Integrodifferential equations and delay models in population dynamics* (Vol. 20). Springer Science & Business Media.

d'Arge, R. C. (1971). Essay on economic growth and environmental quality. *Swedish Journal of Economics*, *73*(1), 25–41.

Dolder, P. J., Minto, C., Guarini, J.-M., & Poos, J. J. (2020). Highly resolved spatiotemporal simulations for exploring mixed fishery dynamics. *Ecological Modelling*, *424*, 109000.

Eide, A. (2018). *Introduction to fisheries economics by the use of Wolfram language and mathematica*. Arne Eide.

El Ouardighi, F., Benchekroun, H., & Grass, D. (2014). Controlling pollution and environmental absorption capacity. *Annals of Operations Research*, *220*(1), 111–133.

Evans, L. C. (2012). *An introduction to stochastic differential equations* (Vol. 82). American Mathematical Society.

Fenichel, N. (1979). Geometric singular perturbation theory for ordinary differential equations. *Journal of Differential Equations*, *31*(1), 53–98.

Ferrara, M., Gori, L., Guerrini, L., & Sodini, M. (2019). A continuous time economic growth model with time delays in environmental degradation. *Journal of Information and Optimization Sciences*, *40*(1), 185–201.

Flaaten, O. (2018). *Fisheries economics and management* (2nd ed.). Ola Flaaten and bookboon.com.

Fonner, R., & Sylvia, G. (2014). Willingness to pay for multiple seafood labels in a niche market. *Marine Resource Economics*, *30*(1), 51–70.

Førsund, F., & Strøm, S. (1980). *Environmental and resource economics (Miljøog ressursøkonomi)*. Universitetsforlaget (in Norwegian).

Frisch, R., & Holme, H. (1935). The characteristic solutions of a mixed difference and differential equation occurring in economic dynamics. *Econometrica: Journal of the Econometric Society*, 225–239.

Garzon, C. A., Rey, M. C., Sarmiento, P. J., & Cardenas, J. C. (2016). Fisheries, fish pollution and biodiversity: Choice experiments with fishermen, traders and consumers. *Economia Politica*, *33*(3), 333–353.

Gazi, N. H., & Bandyopadhyay, M. (2008). Effect of time delay on a harvested predator–prey model. *Journal of Applied Mathematics and Computing*, *26*(1), 263–280.

Gomes, H., Kersulec, C., Doyen, L., Blanchard, F., Cisse, A. A., & Sanz, N. (2021). The major roles of climate warming and ecological competition in the small-scale coastal fishery in French Guiana. *Environmental Modeling & Assessment*, *26*(5), 655–675.

Gori, L., Guerrini, L., & Sodini, M. (2018). Time delays, population, and economic development. *Chaos: An Interdisciplinary Journal of Nonlinear Science*, *28*(5), 055909.

Guckenheimer, J., & Holmes, P. (1983). *Nonlinear oscillations, dynamical systems, and bifurcations of vector fields*. Springer-Verlag.

Guerrini, L., Krawiec, A., & Szydłowski, M. (2020). Bifurcations in an economic growth model with a distributed time delay transformed to ODE. *Nonlinear Dynamics*, *101*(2), 1263–1279.

Haavelmo, T. (1971). The pollution problem from social science point of view (forurensingsproblemet fra samfunnsvitenskapelig synspunkt). *Sosialøkonomen*, (*4*), 5–8 (in Norwegian).

Halpern, B. S., Walbridge, S., Selkoe, K. A., Kappel, C. V., Micheli, F., D'Agrosa, C., Bruno, J. F., Casey, K. S., Ebert, C., Fox, H. E., Fujita, R., Heinemann, D., Lenihan, H. S., Madin, E. M. P., Perry, M. T., Selig, E. R., Spalding, M., Steneck, R., & Watson, R. (2008). A global map of human impact on marine ecosystems. *Science*, *319*(5865), 948–952.

Hannesson, R. (1978). *Economics of fisheries*. Universitetsforlaget.

Heilmann, I. T., Thygesen, U. H., & Sørensen, M. P. (2018). Spatio-temporal pattern formation in predator–prey systems with fitness taxis. *Ecological Complexity*, *34*, 44–57.

Islam, M. S., & Tanaka, M. (2004). Impacts of pollution on coastal and marine ecosystems including coastal and marine fisheries and approach for management: A review and synthesis. *Marine Pollution Bulletin*, *48*(7), 624–649.

Jones, J. C., & Reynolds, J. D. (1997). Effects of pollution on reproductive behaviour of fishes. *Reviews in Fish Biology and Fisheries*, *7*(4), 463–491.

Kar, T., & Chakraborty, K. (2010). Bioeconomic modelling of a prey predator system using differential algebraic equations. *International Journal of Engineering, Science and Technology*, *2*(1), 13–34.

Keeler, E., Spence, M., & Zeckhauser, R. (1971). The optimal control of pollution. *Journal of Economic Theory*, *4*, 19–34.

Keller, A. A. (2010). Generalized delay differential equations to economic dynamics and control. *American-Mathematics*, *10*, 278–286.

Lu, Y., Yuan, J., Lu, X., Su, C., Zhang, Y., Wang, C., Cao, X., Li, Q., Su, J., Ittekkot, V., Garbutt, R. A., Bush, S., Fletcher, S., Wagey, T., Kachur, A., & Sweijd, N. (2018). Major threats of pollution and climate change to global coastal ecosystems and enhanced management for sustainability. *Environmental Pollution*, *239*, 670–680.

Marciniak-Czochra, A., Karch, G., & Suzuki, K. (2017). Instability of turing patterns in reaction–diffusion–ODE systems. *Journal of Mathematical Biology*, *74*(3), 583–618.

Martin, A., & Ruan, S. (2001). Predator–prey models with delay and prey harvesting. *Journal of Mathematical Biology*, *43*(3), 247–267.

Øksendal, B. (2003). Stochastic differential equations. Springer-Verlag.

Perman, R., Ma, Y., Common, M., & McGilvray, J. (2011). *Natural resource and environmental economics* (4th ed.). Pearson.

Ponosov, A., Shindiapin, A., & Miguel, J. (2004). The w-transform links delay and ordinary differential equations. *Functional Differential Equations*, *9*(3–4), 437.

Prieur, F. (2009). The environmental Kuznets curve in a world of irreversibility. *Economic Theory*, *40*(1), 57–90.

Smith, V. L. (1972). Dynamics of waste accumulation: Disposal versus recycling. *The Quarterly Journal of Economics*, *86*(4), 600–616.

Solow, R. M. (1956). A contribution to the theory of economic growth. *The Quarterly Journal of Economics*, *70*(1), 65–94.

Strøm, S. (1971). A simplified analysis of a pollution problem (en forenklet analyse av et forurensingsproblem). *Sosialøkonomen*, (*10*), 23–34 (in Norwegian).

Tietenberg, T., & Lewis, L. (2014). *Environmental and natural resource economics*. Pearson.

Todd, P. A., Ong, X., & Chou, L. M. (2010). Impacts of pollution on marine life in Southeast Asia. *Biodiversity and Conservation*, *19*(4), 1063–1082.

Toman, M. A., & Withagen, C. (2000). Accumulative pollution, "clean technology," and policy design. *Resource and Energy Economics*, *22*(4), 367–384.

Vikas, M., & Dwarakish, G. (2015). Coastal pollution: A review. *Aquatic Procedia*, *4*, 381–388.
Watson, S. C., Paterson, D. M., Queirós, A. M., Rees, A. P., Stephens, N., Widdicombe, S., & Beaumont, N. J. (2016). A conceptual framework for assessing the ecosystem service of waste remediation: In the marine environment. *Ecosystem Services*, *20*, 69–81.
Wessells, C. R., & Anderson, J. G. (1995). Consumer willingness to pay for seafood safety assurances. *Journal of Consumer Affairs*, *29*(1), 85–107.
Whitehead, J. C. (2006). Improving willingness to pay estimates for quality improvements through joint estimation with quality perceptions. *Southern Economic Journal*, *73*(1), 100–111.
William, B., & Xepapadeas, A. (2010). Pattern formation, spatial externalities and regulation in coupled economic-ecological systems. *Journal of Environmental Economics and Management*, *59*(2), 149–164.
Yuan, R., Wang, Z., & Jiang, W. (2016). Global Hopf bifurcation of a delayed diffusive predator–prey model with Michaelis–Menten-type prey harvesting. *Applicable Analysis*, *95*(2), 444–466.
Zhang, Q., Zhang, X., & Liu, C. (2011). A singular bioeconomic model with diffusion and time delay. *Journal of Systems Science and Complexity*, *24*(2), 277–290.
Zhang, Y., Zhang, Q., & Yan, X.-G. (2014). Complex dynamics in a singular Leslie–Gower predator–prey bioeconomic model with time delay and stochastic fluctuations. *Physica A: Statistical Mechanics and its Applications*, *404*, 180–191.

How to cite this article: Bergland, H., Mishra, P., Pedersen, P. A., Ponossov, A., & Wyller, J. (2022). Time delays and pollution in an open-access fishery. *Natural Resource Modeling*, e12363. https://doi.org/10.1111/nrm.12363

APPENDIX A: PERSISTENCY PROPERTY OF THE SYSTEMS (21) AND (22)

Regarding persistency of the solutions of the systems (21) and (22), we have the following result:

Theorem 1. *Consider the systems* (21) *and* (22) *under the assumptions* (23)–(26), *where* $\tilde{f}$ *and* $\tilde{g}$ *are defined in* (27) *and* (28), *respectively*, f *satisfies properties* (*a*) *and* (*b*) *and* ρ *satisfies properties* (*a*)–(*e*) *from Section 2.*

If $\gamma_5 > \gamma_2[pR(0,\gamma_3) + (1-p)R_{\max}]$, *where* $R_{\max} \equiv R(\theta_{\max};\gamma_3)$ *is the maximal value of the function* $R(\theta;\gamma_3)$, $\theta \geq 0$, *then any solution of the systems* (21) *and* (22), *which starts within the region*

$$\begin{aligned}\Sigma = \{(\xi,\eta,\theta,\psi,\langle\theta\rangle,\langle\psi\rangle) :\ & \xi > 0, \eta > 0, \theta > 0, \langle\theta\rangle > 0,\\ & \psi > \gamma_2[pR(0,\gamma_3) + (1-p)R_{\max}], \langle\psi\rangle > 0\},\end{aligned} \tag{A1}$$

remains in Σ *for all* $\tau \geq \tau^*$, *that is*, Σ *is invariant under the solution flow of the systems* (21) *and* (22).

Proof. First of all we notice that

1. If the solution $\psi(\tau)$ of the equation $\psi' = \gamma_4\tilde{f}(\psi;\gamma_5)$, see (36), is positive for some $\tau_0 > 0$, then $\psi(\tau)$ remains positive for all $\tau \geq \tau_0$; any solution $\psi(\tau)$ of this equation approaches the only equilibrium point $\psi = \gamma_5$ of this equation if $\tau \to \infty$.

2. If for some τ_0 the components ξ and η of the solution of the systems (21) and (22) are positive, then they remain positive for all $\tau \geq \tau_0$ even if the other components may be negative.

The first statement follows from the assumption that $\tilde{f}(\psi;\gamma_5) > 0$ *if* $0 \leq \psi < \gamma$ *and* $\tilde{f}(\psi;\gamma_5) < 0$ *if* $\psi > \gamma$. *Therefore,* $\psi(\tau)$ *is strictly increasing on the interval* $0 \leq \psi < \gamma$ *and strictly decreasing on the interval* $\psi > \gamma$. *Thus,* γ_5 *is the global attractor for all solutions* $\psi(\tau)$, *which also cannot cross the line* $\psi = 0$.

The second statement follows from the general properties of dynamical systems of the Lotka–Volterra type, see, for example, Bergland et al. (2019, Appendix B, Lemma 2).

These two facts, together with the observation that the equations for θ and $\langle\theta\rangle$ are independent of ξ, η, and $\langle\psi\rangle$, make it possible to simplify the problem by only considering the subsystem (36). For instance, proving the invariance of the region

$$\Sigma' = \{(\theta, \langle\theta\rangle, \psi) : \ \theta > 0, \langle\theta\rangle > 0, \psi > \gamma_2[pR(0,\gamma_3) + (1-p)R_{\max}]\} \tag{A2}$$

under the solution flow of the subsystem (36) will justify the statement of Theorem 1.

Let $P^* = (\theta(\tau^*), \langle\theta\rangle(\tau^*), \psi(\tau^*)) \in \Sigma$ for some $\tau^* \leq 0$. Assume that there exists $\tau_1 > \tau^*$ such that the trajectory, which starts at P^* hits the boundary $\partial\Sigma'$ of the region Σ' at τ_1 for the first time. Evidently, the trajectory cannot hit the face

$$\{\psi = \gamma_2[pR(0,\gamma_3) + (1-p)R_{\max}], \theta \geq 0, \langle\theta\rangle \geq 0\}$$

of $\partial\Sigma'$, because the component $\psi(\tau)$ of the solution monotonically approaches $\gamma_5 \geq \gamma_2[pR(0,\gamma_3) + (1-p)R_{\max}] > \psi(\tau^*)$. Therefore, it must be either the face

$$\{\theta = 0, \langle\theta\rangle \geq 0, \psi \geq \gamma_2[pR(0,\gamma_3) + (1-p)R_{\max}]\} \tag{A3}$$

or the face

$$\{\langle\theta\rangle = 0, \theta \geq 0, \psi \geq \gamma_2[pR(0,\gamma_3) + (1-p)R_{\max}]\}. \tag{A4}$$

If the trajectory hits the face (A3) at $\tau = \tau_1$, then $\theta'(\tau_1) \leq 0$, because $\theta(\tau_1) = 0$ and $\theta(\tau) > 0$ for $\tau^* < \tau < \tau_1$. On the other hand, $\langle\theta\rangle(\tau_1) \geq 0$, and we obtain

$$\begin{aligned}\theta'(\tau_1) &= \psi(\tau_1) - \gamma_2[pR(\theta(\tau_1),\gamma_3) + (1-p)R(\langle\theta\rangle(\tau_1),\gamma_3)] \\ &= \psi(\tau_1) - \gamma_2[pR(0,\gamma_3) + (1-p)R(\langle\theta\rangle(\tau_1),\gamma_3)] \\ &\geq \psi(\tau_1) - \gamma_2[pR(0,\gamma_3) + (1-p)R_{\max}] > 0,\end{aligned}$$

which contradicts the property $\theta'(\tau_1) \leq 0$. Hence, the trajectory never hits the face (A3) of the boundary $\partial\Sigma'$.

Finally, if the trajectory hits the face (A4) at $\tau = \tau_1$, then $\langle\theta\rangle'(\tau_1) = \gamma(\theta(\tau_1) - \langle\theta\rangle(\tau_1)) \leq 0$, because $\langle\theta\rangle(\tau_1) = 0$ and $\langle\theta\rangle(\tau) > 0$ for $\tau^* < \tau < \tau_1$. Therefore, $0 \leq \theta(\tau_1) \leq \langle\theta\rangle(\tau_1) = 0$, so that $\theta(\tau_1) = 0$, which means that the trajectory hits the face (A3), which is impossible. Hence the theorem is proved. □

We conclude this section with two remarks.

1. If $p = 1$ (no delay in the variable θ), then Theorem 1 converts to Theorem 1 in Bergland et al. (2019).
2. Under assumptions of Theorem 1, all components of the solution of the systems (21) and (22) remain positive, once the initial values of all components are positive. This ensures the property of persistence of the model. However, if the condition (A1) is violated, then the component θ may become negative after a finite time, so that the model is not persistent. This is, for example, always the case if $p = 1$ (no delay in the variable θ), see Bergland et al. (2019, Appendix B, Lemma 1).

APPENDIX B: SLOW–FAST ANALYSIS OF THE ECONOMIC-GROWTH AND POLLUTION BLOCK OF THE MODELING FRAMEWORK

Following Fenichel (1979) we first rescale the problem (36) by means of the transformation:

$$\begin{aligned} s = \tau/\varepsilon_\gamma, \quad \Lambda(s) = \xi(\tau), \quad \Upsilon(s) = \eta(\tau), \quad \Theta(s) = \theta(\tau), \\ \Psi(s) = \psi(\tau), \quad \langle\Theta\rangle(s) = \langle\theta\rangle(\tau). \end{aligned} \tag{B1}$$

Here s is the fast time scale. We readily find that

$$\begin{cases} \dot{\Theta} = \epsilon_\gamma \mathcal{H}(\Lambda, \Upsilon, \Theta, \Psi, \langle\Theta\rangle, \langle\Psi\rangle), \\ \dot{\Psi} = \epsilon_\gamma \mathcal{K}(\Lambda, \Upsilon, \Theta, \Psi, \langle\Theta\rangle, \langle\Psi\rangle), \\ \langle\dot{\Theta}\rangle = \mathcal{A}(\Lambda, \Upsilon, \Theta, \Psi, \langle\Theta\rangle, \langle\Psi\rangle), \end{cases} \tag{B2}$$

where $\dot{}$ denotes the derivative with respect to fast variable s. Letting $\epsilon_\gamma \to 0$ in (35) and (B2) we get the following DAE:

$$\begin{cases} \theta' = \mathcal{H}(\xi, \eta, \theta, \psi, \langle\theta\rangle) = \psi - \gamma_2[pR(\theta; \gamma_3) + (1-p)R(\langle\theta\rangle; \gamma_3)], \\ \psi' = \mathcal{K}(\xi, \eta, \theta, \psi, \langle\theta\rangle, \langle\psi\rangle) = \gamma_4 \tilde{f}(\psi; \gamma_5), \\ 0 = \mathcal{A}(\xi, \eta, \theta, \psi, \langle\theta\rangle, \langle\psi\rangle) \end{cases} \tag{B3}$$

and the following reduced fast subsystem containing the fast variables only, that is,

$$\dot{\Theta} = 0, \quad \dot{\Psi} = 0, \quad \langle\dot{\Theta}\rangle = \mathcal{A}(\Lambda, \Upsilon, \Theta, \Psi, \langle\Theta\rangle\langle\Psi\rangle), \tag{B4}$$

where Θ and Ψ are regarded as parameters. The system (B4) is also referred to as the layered system. Both the systems (B3) and (B4) capture some information of the full system, but with limited validity in phase space and time. However, a global picture of the dynamics can be retrieved by matching the solutions of both systems. Now we apply the singular perturbation theory that defines the slow manifold of (B2) as the equilibrium of the fast subsystem (B4). This manifold is given as the 2D subspace $\mathcal{M}^a$ defined by means of (48). $\mathcal{M}^a$ is also referred to as a *critical manifold* or a *critical surface*. Following Fenichel's theory (Fenichel, 1979) we first check the hyperbolicity of the critical manifold. Now to have hyperbolicity we derive stability of equilibrium points of the fast subsystem we have $\mathcal{A}_{\langle\theta\rangle}(\xi, \eta, \theta, \psi, \langle\theta\rangle, \langle\psi\rangle)|_{\langle\theta\rangle=\theta} = -1$. Therefore M^a is normally attracting hyperbolic manifold. Hence for a small $\varepsilon_\gamma > 0$, there exists an

invariant manifold $\mathcal{M}_\varepsilon^a$ for the system (B4) which implies the persistence of the slow manifold $\mathcal{M}^a$. The slow manifold $\mathcal{M}_{\varepsilon_\gamma}^a$ has the same smoothness and stability properties of the critical manifold $\mathcal{M}^a$. Therefore for a small sufficiently small $\varepsilon_\gamma > 0$, the flow on perturbed slow manifold $\mathcal{M}_{\varepsilon_\gamma}^a$ is diffeomorphic to the associated flow on the critical manifold $\mathcal{M}^a$.

Let us discuss the slow–fast dynamics of the limiting slow system (B3) in terms of dynamical system theory. On the slow surface M^a (defined by Equation 48) the dynamical evolution of slow variables θ and ψ is governed by means of the 2D subsystem (38). One can easily verify that the dynamical evolution of slow variables associated with the DAE problem (B3) on the critical manifold M^a matches the dynamical behavior of the 2D subsystem (38).

We then combine the results obtained for the two limiting systems (B3) and (B4) to conclude about the properties of the slow–fast subsystem (B2). The above analysis suggests that accumulating the perturbation parameter ε_γ from zero to a small finite value does not destroy the geometric properties which are related to the qualitative dynamics of the layered and the reduced system. The layered problem captures the fast progression of the dynamic variable $\langle\theta\rangle$ towards (or away from) the slow manifold $\mathcal{M}^a$ whereas the reduced problem (B3) yields a good approximation of the slow progression of the variables θ and ψ on the attracting critical manifold $\mathcal{M}^a$. Figure B1 summarizes the geometrical interpretation of the results discussed above.

Finally we consider the scenario with the separation of time scales $T_\mu \ll T_\gamma \ll T_r$, which means that $\varepsilon_\mu \ll \varepsilon_\gamma \ll 1$, where $\varepsilon_\mu = T_\mu/T_r = r/\mu$, $\varepsilon_\gamma = T_\gamma/T_r = r/\gamma$. We conveniently express this time separation in terms of $\varepsilon \equiv \frac{\gamma}{\mu} = \frac{T_\mu}{T_\gamma} \ll 1$ from which it follows that $\varepsilon_\mu = \varepsilon_\gamma \varepsilon$. The dynamical evolution decomposes into three phases in this case: In the first phase we have a rapid attraction of the integral curves of (35) towards the 3D subspace $\mathcal{M}^b$ of $\mathbb{R}^4$ defined as

$$\begin{aligned}\mathcal{M}^b &= \{(\theta, \psi, \langle\theta\rangle, \langle\psi\rangle) \in \mathbb{R}^4 : \mathcal{B}(\xi, \eta, \theta, \psi, \langle\theta\rangle, \langle\psi\rangle) = 0\} \\ &= \{(\theta, \psi, \langle\theta\rangle, \langle\psi\rangle) \in \mathbb{R}^4 : \langle\psi\rangle = \psi\}\end{aligned}$$

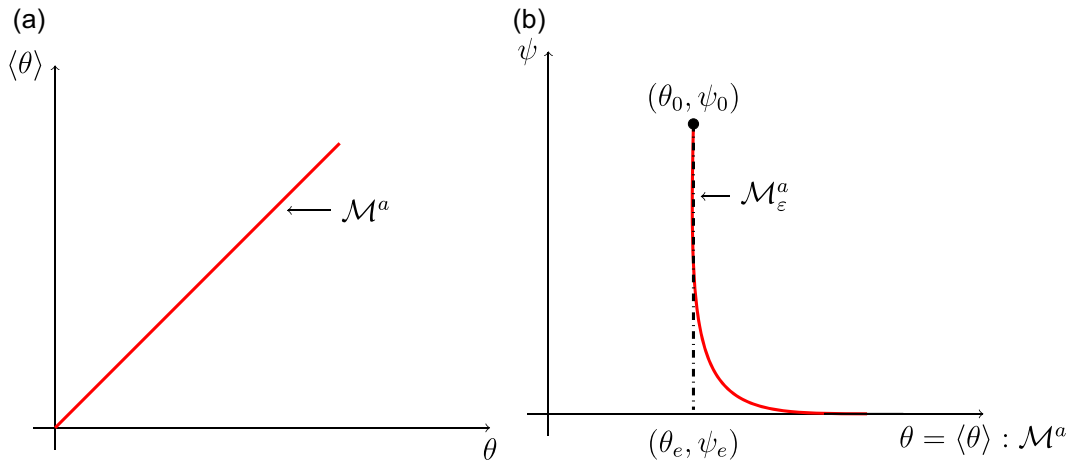

FIGURE B1 (a) Geometrical interpretation of the one-dimensional attracting slow manifold $\mathcal{M}^a$ of the layer system (B4). (b) An invariant manifold $\mathcal{M}_\varepsilon^a$ implies the persistence of the slow manifold $\mathcal{M}^a$.

asymptotically as $\varepsilon_\mu \to 0$. Notice that the other state variables remain constant in this asymptotic limit. In the second intermediate phase the dynamical evolution will take place on $\mathcal{M}^b$. This result follows from the fact that $\mathcal{M}^b$ always is an attracting normally hyperbolic manifold of the subsystem (35). The dynamical evolution on $\mathcal{M}^b$ is governed by means of the 3D system (B2), which is as shown in the previous paragraph a singularly perturbed system in its own right with ε_γ as a perturbation parameter. The outcome of the analysis of this system in the asymptotic limit $\varepsilon_\gamma \to 0$ goes as follows: The system (B2) predicts that we have a rapid attraction described by means of (B4) of the integral curves towards the subspace $\mathcal{M}^a$ of $\mathcal{M}^b$ of the mean value $\langle\theta\rangle$ in which the remaining state variables θ and ψ are constant, followed by a temporal evolution on $\mathcal{M}^a$ by means of the 2D system (36).

APPENDIX C: SLOW–FAST ANALYSIS ON THE TIME SCALE $T_\mu \sim T_\gamma \ll T_r$ OF THE MODELING FRAMEWORK

Here we assume the time-scale separation $T_\mu \sim T_\gamma \ll T_r$ which means that $\mu \sim \gamma \gg r$ which gives $\varepsilon_\mu \sim \varepsilon_\gamma$. For the sake of simplicity we put $T_\mu = T_\gamma (\Leftrightarrow \mu = \gamma)$ in our calculations. In this case the system of interest is given as

$$\begin{aligned} \xi' &= \xi\mathcal{F}(\xi,\eta,\theta,\psi,\langle\theta\rangle,\langle\psi\rangle), \quad \eta' = \eta\mathcal{G}(\xi,\eta,\theta,\psi,\langle\theta\rangle,\langle\psi\rangle),\\ \theta' &= \mathcal{H}(\xi,\eta,\theta,\psi,\langle\theta\rangle,\langle\psi\rangle), \quad \psi' = \mathcal{K}(\xi,\eta,\theta,\psi,\langle\theta\rangle,\langle\psi\rangle),\\ \varepsilon_\gamma\langle\theta\rangle' &= \theta - \langle\theta\rangle, \varepsilon_\gamma\langle\psi\rangle' = \psi - \langle\psi\rangle, \end{aligned} \tag{C1}$$

where $\mathcal{F}, \mathcal{G}, \mathcal{H}, \mathcal{K}$ are defined in (21). Here $'$ denotes derivative with respect to τ. We rescale the system (C1) to the dynamical system

$$\begin{aligned} \dot\Lambda &= \varepsilon_\gamma\Lambda\mathcal{F}(\Lambda,\Upsilon,\Theta,\Psi,\langle\Theta\rangle,\langle\Psi\rangle), \quad \dot\Upsilon = \varepsilon_\gamma\Upsilon\mathcal{G}(\Lambda,\Upsilon,\Theta,\Psi,\langle\Theta\rangle,\langle\Psi\rangle),\\ \dot\Theta &= \varepsilon_\gamma\mathcal{H}(\Lambda,\Upsilon,\Theta,\Psi,\langle\Theta\rangle,\langle\Psi\rangle), \quad \dot\Psi = \varepsilon_\gamma\mathcal{K}(\Lambda,\Upsilon,\Theta,\Psi,\langle\Theta\rangle,\langle\Psi\rangle),\\ \langle\dot\Theta\rangle &= \Theta - \langle\Theta\rangle, \quad \langle\dot\Psi\rangle = \Psi - \langle\Psi\rangle, \end{aligned} \tag{C2}$$

where the fast time variable s and the state variables $(\Lambda, \Upsilon, \Theta, \Psi, \langle\Theta\rangle, \langle\Psi\rangle)$ are defined by (B1). Here $\dot{}$ denotes the derivative with respect to the variable s. Equations (C1) and (C2) are referred to as the slow and fast systems, respectively. Notice that (C1) is equivalent with (C2) for $\varepsilon_\gamma > 0$. When letting $\varepsilon_\gamma = 0$ in (C1) and (C2) we get the reduced DAEs:

$$\begin{aligned} \xi' &= \xi\mathcal{F}(\xi,\eta,\theta,\psi,\langle\theta\rangle,\langle\psi\rangle), \quad \eta' = \eta\mathcal{G}(\xi,\eta,\theta,\psi,\langle\theta\rangle,\langle\psi\rangle),\\ \theta' &= \mathcal{H}(\xi,\eta,\theta,\psi,\langle\theta\rangle,\langle\psi\rangle), \quad \psi' = \mathcal{K}(\xi,\eta,\theta,\psi,\langle\theta\rangle,\langle\psi\rangle),\\ \langle\theta\rangle &= \theta, \quad \langle\psi\rangle = \psi, \end{aligned} \tag{C3}$$

and the layered system

$$\begin{aligned} \dot\Lambda = 0, \quad \dot\Upsilon = 0, \quad \dot\Theta = 0, \quad \dot\Psi = 0,\\ \langle\dot\Theta\rangle = \Theta - \langle\Theta\rangle, \quad \langle\dot\Psi\rangle = \Psi - \langle\Psi\rangle. \end{aligned} \tag{C4}$$

Our main aim is to analyze (C3) and (C4) by applying geometric perturbation theory. We first observe that the reduced system (C3) predicts that the dynamical evolution takes place in the four dimensional subspace $\mathcal{M}_0$ of $\mathbb{R}^6$ defined by means of (66). $\mathcal{M}_0$ is also referred to as the

slow manifold or *critical manifold* (Fenichel, 1979). Notice the role of $\mathcal{M}_0$: It plays the role as the equilibrium state of the subsystem

$$\langle \dot{\Theta} \rangle = \Theta - \langle \Theta \rangle, \quad \langle \dot{\Psi} \rangle = \Psi - \langle \Psi \rangle$$

of (C4). On the fastest time scale, the state variables ξ, η, θ, and ψ are constant, in accordance with the system (C4). The slow manifold $\mathcal{M}_0$ is a normally attracting hyperbolic manifold. From Fenichel's first theorem it follows that for a small $\varepsilon_\gamma > 0$, there exists a invariant manifold $\mathcal{M}_{\varepsilon_\gamma}$ for the system (C1) which implies the persistence of the slow manifold $\mathcal{M}_0$. The slow manifold $\mathcal{M}_{\varepsilon_\gamma}$ has the same smoothness and stability properties of critical manifold $\mathcal{M}_0$. Therefore the flow on the perturbed slow manifold is diffeomorphic to the associated slow flow on the critical manifold for sufficiently small ε_γ (Fenichel, 1979).